

ORIGINS OF ECCENTRIC EXTRASOLAR PLANETS: TESTING THE PLANET–PLANET SCATTERING MODEL

ERIC B. FORD^{1,2,3} AND FREDERIC A. RASIO⁴
to accepted in ApJ

ABSTRACT

In planetary systems with two or more giant planets, dynamical instabilities can lead to collisions or ejections through strong planet–planet scattering. Previous studies for simple initial configurations with two equal-mass planets revealed two discrepancies between the results of numerical simulations and the observed orbital elements of extrasolar planets: the potential for frequent collisions between giant planets and a narrow distribution of final eccentricities following ejections. Here, we show that simulations with two *unequal mass* planets starting on nearly circular orbits predict a reduced frequency of collisions and a broader range of final eccentricities. We show that the two-planet scattering model can easily reproduce the observed eccentricities with a plausible distribution of planet mass ratios. Further, the two-planet scattering model predicts a maximum eccentricity of $\simeq 0.8$, independent of the distribution of planet mass ratios, provided that both planets are initially place on nearly circular orbits. This compares favorably with current observations and will be tested by future planet discoveries. Moreover, we show that the combination of planet–planet scattering and tidal circularization may be able to explain the existence of some giant planets with very short period orbits. Orbital migration due to planet scattering could play an important role in explaining the increased rate of giant planets with orbital periods of less than a year, as found by radial velocity surveys. We also re-examine and discuss various possible correlations between eccentricities and other properties of observed extrasolar planets. We find that the radial velocity observations are consistent with planet eccentricities being correlated with the ratio of the escape velocity from the planet’s surface relative to the escape velocity from the host star at the planet’s location. We demonstrate that the observed distribution of planet masses, orbital periods, and eccentricities can provide constraints for models of planet formation and evolution.

Subject headings: planetary systems — planetary systems: formation — planets and satellites: general — celestial mechanics

1. INTRODUCTION

For several centuries, theories of planet formation had been designed to explain our own Solar System, but the first few discoveries of extrasolar planets immediately sent theorists back to the drawing board. These discoveries led to the realization that planet formation theory must be generalized to explain a much wider range of properties for planetary systems. For example, it had long been assumed that planets formed in circular orbits because of strong eccentricity damping in the proto-planetary disk and that their orbits would later remain nearly circular (i.e., with eccentricity $e \leq 0.1$; Lissauer 1993, 1995). However, over half of the extrasolar planets beyond 0.1 AU have eccentricities $e \geq 0.3$, and two have eccentricities larger than 0.9.

The planets in eccentric orbits are generally believed to have formed on nearly circular orbits but later evolved to their presently observed large eccentricities. Theorists have suggested numerous mechanisms to excite the orbital eccentricity of giant planets. These include:

- a) secular perturbations due to a distant stellar or massive planetary companion (Holman, Touma, & Tremaine 1997; Mazeh et al. 1997; Ford, Kozinsky, & Rasio 2000; Takeda & Rasio 2005),
- b) perturbations from passing stars (Laughlin & Adams 1998; Hurley & Shara 2002; Zakamska & Tremaine 2004),
- c) strong planet–planet scattering events in planetary systems with either a few planets (Rasio & Ford 1996; Weidenschilling & Marzari 1996; Ford, Havlickova, & Rasio 2001 (FHR); Marzari & Weidenschilling 2002; Yu & Tremaine 2001; Ford, Rasio & Yu 2003; Veras & Armitage 2004, 2005, 2006) or many planets (Lin & Ida 1997; Levison et al. 1998; Papaloizou & Terquem 2001; Adams & Laughlin 2003; Moorhead & Adams 2005; Goldreich, Lithwick, & Sari 2004; Ford & Chiang 2007; Juric & Tremaine 2008),
- d) interactions of orbital migration with mean-motion resonances (Chiang & Murray 2002; Kley 2000; Kley et al. 2004, 2005; Lee & Peale 2002; Tsiganis et al. 2005),
- e) resonances between secular perturbations and precession induced by general relativity, stellar oblateness, and/or a remnant disk (Ford et al. 2000; Nagasawa et al. 2003; Adams & Laughlin 2006),

Electronic address: eford@astro.ufl.edu

¹ Department of Astronomy, University of Florida, 211 Bryant Space Science Center, P.O. Box 112055, Gainesville, FL 32611-2055

² Hubble Fellow

³ Harvard-Smithsonian Center for Astrophysics, Mail Stop 51, 60 Garden Street, Cambridge, MA 02138

⁴ Department of Physics and Astronomy, Northwestern University, Evanston, IL 60208

- f) interactions with a planetesimal disk (Murray et al. 1998),
- g) interactions with a gaseous proto-planetary disk (Goldreich & Tremaine 1980; Artymowicz 1992; Papaloizou & Larwood 2000; Papaloizou et al. 2001; Goldreich & Sari 2003; Ogilvie & Lubow 2003; Cresswell et al. 2007; Moorhead & Adams 2008),
- h) asymmetric stellar jets (Namouni 2005, 2006), and
- i) hybrid scenarios that combine aspects of more than one of the above mechanisms (e.g., Marzari et al. 2005; Sandor & Kley 2006; Malmberg et al. 2007ab).

Some of mechanisms (a, b) inevitably influence the evolution of some planetary systems, but are not able to explain the ubiquity of eccentric giant planets (Zakamska & Tremaine 2004; Takeda & Rasio 2005). Observations of multiple planet systems have provided strong evidence that other mechanisms (c, d) are also significant in altering planet's orbital eccentricities. For example, the dramatic eccentricity oscillations of ν And c provide an upper limit on the timescale for eccentricity excitation in ν And ($\simeq 100$ yr) and strong evidence for planet-planet scattering in this system (Ford, Lystad & Rasio 2005). Other multiple planet systems may also exhibit similar behavior (Barnes & Greenberg 2006ab). Simulations of possible progenitors to our own outer solar system have shown that instabilities can be postponed while there is a significant disk mass and become manifest once the mass of the disk decreases (relative to the planets' mass). Further, the remaining disk need not be sufficiently massive to damp the eccentricities of eccentric planets that emerge from the instability (Ford & Chiang 2007; Chatterjee et al. 2008). As another example, the detection of pairs of planets in 2:1 mean motion resonances (e.g., GJ 876 b & c) suggests that smooth convergent migration likely occurred in these systems. Additionally, the fact that migration models can simultaneously match the observed eccentricities for both planets b & c suggests eccentricity excitation was related to the migration and resonant capture in this system (Lee & Peale 2002; Kley et al. 2005). It is not clear if the remaining mechanisms (e-h) are important for shaping the actual distribution of planet eccentricities.

In this paper, we expand upon the original planet-planet scattering model of Rasio & Ford (1996) and FHR. First, we evaluate some potential origins of dynamical instabilities that result in close encounters and strong planet-planet scattering in §2. In §3, we present the results of n -body simulations of planet-planet scattering for systems with two giant planets of unequal masses. Then, in §4, we compare the predictions of eccentricity excitation models with the eccentricities of the known extrasolar planets. In §5, we discuss the implications of our work for theories of eccentricity excitation and damping and suggest how future observations can further test theories for eccentricity excitation.

2. ORIGIN OF INSTABILITY

While some authors have simulated multiple planet systems beginning with the planet formation stage, computational cost has limited such simulations to a small

portion of the disk and/or small number of initial conditions (e.g., Kokubo & Ida 1998; Levison, Lissauer, & Duncan 1998). Since dynamically unstable planetary systems are highly chaotic, we can only investigate the statistical properties of an ensemble of systems with similar initial conditions. Thus, most investigations of dynamical instabilities in multiple planet systems proceed by simulating systems after planets have formed and perturbations due to the protoplanetary disk are no longer significant. The planets are placed on plausible initial orbits and numerically integrated according to the gravitational potential of the central star and other planets.

Clearly, the choice of initial conditions will determine whether the systems are dynamically stable and will affect the outcome of unstable systems. Our simulations of planet-planet scattering typically begin with closely spaced giant planets (e.g., Rasio & Ford 1996; FHR). This is necessary for dynamical instabilities to occur in systems with only two planets initially on circular orbits. For two-planet systems, there is a sharp transition from rigorous Hill stability to chaos and strong interactions. Therefore, one potential concern about the relevance of dynamical instabilities is whether the necessary initial conditions will manifest themselves in the two-planet configurations that occur in nature. In this section, we describe several possible mechanisms that could lead to dynamical instabilities in two-planet systems, including mass growth through accretion, dissipation of the protoplanetary disk, and orbital migration. Additionally, the secular evolution of systems with more than two planets provides a natural mechanism for triggering dynamical instabilities, even long after the protoplanetary disk has dissipated and planets are fully assembled (Chatterjee et al. 2008).

According to the standard core accretion model, once a rocky planetary core reaches a critical mass, it rapidly accretes the gas within its radius of influence in a circumstellar disk. Thus, the semi-major axis of a planetary core is determined by the collisional evolution of protoplanets, while the mass of a giant planet is determined by the state of the gaseous disk when the core reaches the critical mass (Lissauer 1993). Two planetary cores could form with an initial separation sufficient to prevent close encounters while their masses are less than the critical mass for runaway accretion, but insufficient to prevent a dynamical instability after the onset of rapid mass growth due to gas accretion (Pollack et al. 1996). For closely packed massive giant planets, the final stage of mass growth may occur via accretion through a common gap (e.g., Schafer et al. 2004; Sandor et al. 2007).

The accumulation of random velocities provides another possible source of a dynamical instability. Assuming planets form in the presence of a dissipative disk, they are expected to form on nearly circular and coplanar orbits. While the timescale for dissipation in the disk remains shorter than the timescales for eccentricity excitation, eccentricities and inclinations will be damped, preventing close encounters. Both analytical and numerical studies of eccentricity damping in gaseous disks suggest that the eccentricity damping timescale is much shorter than the migration timescale (Goldreich & Tremaine 1980; Trilling et al. 1998; Nelson et al. 2000; Papaloizou et al. 2001). According to a dynamical analysis of the GJ 876 multiple planet systems, the current ec-

centricities suggests that eccentricity damping timescale must have been at least 40 times more rapid than the migration timescale (Lee & Peale 2002; Kley et al. 2005). Thus, planets are assumed to remain on nearly circular orbits during putative early migration stage. As the disk dissipates, eccentricity damping becomes less significant, so mutual planetary perturbations can excite significant eccentricities and inclinations and lead to close encounters between planets. Since the photoevaporation timescale ($\sim 10^5$ yr; Alexander et al. 2006) is often much shorter than the timescale for dynamical instabilities to arise, the outcome of the instabilities are expected to be insensitive to the details of the photoevaporation process. We have begun to investigate the dynamical evolution of multi-planet systems that are interacting with a gas disk in order to test this assertion and to better understand the implications of trapping in mean motion resonances for the onset of dynamical instabilities (Chatterjee et al. 2008; Payne et al. in prep). The results of such simulations are beyond the scope of this paper and will be reported in future papers.

Finally, the discovery of giant planets at small orbital separations suggests that orbital migration may be common. In multiple planet systems, convergent migration (i.e., with the ratio of semi-major axes approaching unity) could increase the strength of mutual planetary perturbations and excite eccentricities (even before/without resonant capture). For systems with exactly two giant planets, then the stability boundary (assuming nearly circular orbits) occurs inside the 2:1 mean motion resonance. Therefore, if systems form with a ratio of orbital periods exceeding 2:1, then a smooth migration would be expected to result in capture into the 2:1 mean motion resonance. Continued migration is expected to result in significant eccentricity excitation (e.g., Lee & Peale 2002). Indeed, this can lead to the onset of dynamical instabilities and strong planet-planet scattering (e.g., Sandor & Kley 2006; Sandor et al. 2007). Similar outcomes may occur due to trapping in the other mean motion resonances (e.g., 3:1, Adams & Laughlin 2003; 3:2 or perhaps 5:3, Lee et al. 2008). Our choice of initial conditions in this paper is not intended to represent this scenario. We intend to explore this scenario in future investigations.

In contrast to the case of two-planet systems, there is no sharp stability criterion for three-planet systems. Three-planet systems can be unstable even for initial orbital spacings significantly greater than would be necessary for similar two-planet systems to be unstable (Chambers, Wetherill & Boss 1996). Additionally, such systems can evolve quasi-stably for very long times, $\sim 10^6 - 10^{10}$ yr, before chaos finally leads to close encounters and strong planet-planet scattering (Marzari & Weidenschilling 2002; Chatterjee et al. 2008). This longer timescale until close encounters could allow sufficient time for three or more planets to form via either the disk instability or core accretion models.

If protoplanetary disks form many planets nearly simultaneously, then planet-planet scattering may lead to a phase of dynamical relaxation. Several researchers have numerically investigated the dynamics of planetary systems with $\sim 10 - 100$ planets (Lin & Ida 1997; Levison et al. 1998; Papaloizou & Terquem 2001, 2002; Adams & Laughlin 2003; Barnes & Quinn 2004; Juric & Tremaine

2008; Payne et al. in prep). Initially, such systems are highly chaotic and close encounters are common. The close encounters lead to planets colliding (creating a more massive planet) and/or planets being ejected from the system, depending on the orbital periods and planet radii. Either process results in the number of planets in the system being reduced and the typical separations between planets increasing. The system gradually evolves from a highly unstable state to quieter states, which can last longer before the next collision or ejection. Such systems typically evolve ultimately to a final state with 1–3 eccentric giant planets that will persist for the lifetime of the star (Adams & Laughlin 2003; Juric & Tremaine 2008).

With so many possibilities for triggering dynamical instabilities in multiple planet systems, we expect that these processes may be rather ubiquitous. While real planetary systems likely have more than two massive bodies, simulations of relatively simple systems (e.g., with just two giant planets) facilitate the systematic study of the relevant physics and help develop intuition for thinking about the evolution of more complex systems.

3. NUMERICAL INVESTIGATION OF PLANET-PLANET SCATTERING

In the previous section, we argued that if planet formation commonly results in planetary systems with multiple planets, then it should be expected that the initial configurations will not be dynamically stable for time spans orders of magnitude longer than the timescale for planet formation. Shortly after the discovery of the first eccentric extrasolar planets, Rasio & Ford (1996) conducted Monte Carlo integrations of planetary systems containing two equal-mass giant planets initially placed just inside the Hill stability limit (Gladman 1993). They numerically integrated the orbits of such systems until there was a collision, or one planet was ejected from the system, or some maximum integration time was reached. The two most common outcomes were collisions between the two planets, producing a more massive planet in a nearly circular orbit between the two initial orbits, and ejections of one planet from the system while the other planet remains in a tighter orbit with a large eccentricity. The relative frequency of these two outcomes depends on the ratio of the escape velocity from the surface of the planet to the escape velocity from the host stars at the planet's location (see §4.3.3).

While this model could naturally explain how planets acquire large eccentricities, FHR performed a large ensemble of planet-planet scattering experiments to compare the resulting planetary systems to the observed sample and found two important differences. First, for the relevant radii and semi-major axes, collisions of Jupiter-mass planets were more frequent in the simulations than nearly circular orbits are observed among the known extrasolar planets.

However, the branching ratios from those simulations may not be appropriate for realistic planetary systems. Since there is a sharp and rigorous Hill stability limit for two-planet systems, the initial conditions placed the two planets in orbits with a relatively small separation. Since FHR also assigned the planets small initial eccentricities and inclinations, the planets initially had a small rela-

tive velocity at conjunction (compared to their circular velocity) and gravitational focusing increased the rate of collisions early on in the simulations. The rate of collisions drops significantly (for the systems that survive long enough) once the planets have had time to excite each other’s eccentricities. Thus, the fraction of systems that result in collisions is likely sensitive to the initial conditions.

To determine more accurately the fraction of actual two-planet systems that result in collisions, future studies would need to model the onset of the instability more realistically. Unfortunately, direct n -body integrations of young planetary systems with small bodies are extremely computationally demanding. The significance of initial conditions is less pronounced for n -body integrations of systems with three or more planets, since more distant initial spacings can be used, so that all close encounters occur only after the planets have excited each other’s eccentricities. Despite these potential complications, it can be useful to study relatively simple model systems to develop intuition for more complex problems and to understand the limitations of simple models. In that spirit, FHR reported the results of planet–planet scattering experiments involving two equal-mass planets, while here we report the results of planet–planet scattering experiments involving two planets of unequal masses.

The more significant shortcoming of the two equal-mass planet scattering model identified by FHR was that, in systems leading to one ejection, the eccentricity distribution of the remaining planet was concentrated in a narrow range and was greater than the typical eccentricity of the known extrasolar planets (See Fig. 3, right, rightmost curve). FHR speculated that planet–planet scattering involving two planets of unequal masses would result in planets remaining with a broader distribution of eccentricities. In this section, we present results that confirm this speculation and quantify the resulting eccentricities.

3.1. Initial Conditions

We used the mixed variable symplectic algorithm of Wisdom & Holman (1991), modified to allow for close encounters between planets as implemented in the publicly available code *Mercury* (Chambers 1999). The results presented below are based on $\sim 10^4$ numerical integrations. Our numerical integrations were performed for a system containing two planets, with mass ratios $10^{-4} < \mu_i < 10^{-2}$, where $\mu_i \equiv m_i/M_*$, m_i is the mass of the i th planet, and M_* is the mass of the central star. We use $i = 1$ to denote the planet initially closer to the star and $i = 2$ to denote the planet initially more distant from the star. A mass ratio of $\mu_i \simeq 10^{-3}$ corresponds to $m \simeq 1 M_{\text{Jup}}$ for $M = 1 M_{\odot}$, where M_{Jup} is the mass of Jupiter and M_{\odot} is the mass of the sun. The initial semimajor axis of the inner planet ($a_{1,\text{init}}$) was set to unity and the initial semimajor axis of the outer planet ($a_{2,\text{init}}$) was drawn from a uniform distribution ranging from $0.9 \cdot a_{1,\text{init}} (1 + \Delta_c)$ to $a_{1,\text{init}} (1 + \Delta_c)$, where $1 + \Delta_c$ is the critical semi-major axis ratio above which Hill stability is guaranteed for initially circular coplanar orbits, and $\Delta_c \simeq 2.4 \times (\mu_1 + \mu_2)^{1/3}$ (Gladman 1993). For small non-zero eccentricities, some of our initial conditions will result in stable planetary systems. If we were to cal-

culate branching ratios for collisions or ejections relative to the total number of simulations, then our results would depend slightly on our choice of initial conditions. Therefore, we present the fractions of systems that have a certain property, conditioned on there being an ejection. When presented in this form, our results are insensitive to the number of systems that remained bound and whether they were chaotic.

The initial eccentricities were distributed uniformly in the range from 0 to 0.05, and the initial relative inclination in the range from 0° to 2° . All remaining angles (longitudes and phases) were randomly chosen between 0 and 2π . Throughout this paper we quote numerical results in units such that $G = a_{1,\text{init}} = M_* = 1$, where G is the gravitational constant. In these units, the initial orbital period of the inner planet is $P_1 \simeq 2\pi$.

Throughout the integrations, close encounters between any two bodies were logged, allowing us to use a single set of n -body integrations to study the outcome of systems with a wide range of planetary radii. We consider a range of radii to allow for the uncertainty in both the physical radius and the effective collision radius allowing for dissipation in the planets. When two planets collided, mass and momentum conservation were assumed to compute the final orbit of the resulting single planet.

Each run was terminated when one of the following four conditions was encountered: (i) one of the two planets became unbound (which we defined as having a radial distance from the star of $2000 a_{1,\text{init}}$); (ii) a collision between the two planets occurred assuming $R_i/a_{1,\text{init}} = R_{\text{min}}/a_{1,\text{init}} = 1 R_{\text{Jup}}/5 \text{ AU} = 0.95 \times 10^{-4}$, where R_{Jup} is the radius of Jupiter; (iii) a close encounter occurred between a planet and the star (defined by having a planet come within $r_{\text{min}}/a_{1,\text{init}} = 10 R_{\odot}/5 \text{ AU} = 0.01$ of the star); (iv) the integration time reached $t_{\text{max}} = 5 \cdot 10^6 - 2 \cdot 10^7$ depending on the masses of the planets. These four types will be referred to as “collisions,” meaning a collision between the two planets, “ejections,” meaning that one planet was ejected to infinity, “star grazers,” meaning that one planet had a close pericenter passage, and “two planets.”

3.2. Results

We began by conducting an exploratory set of integrations using a wide variety of planet masses ($10^{-3} \leq \mu_i < 10^{-2}$). The probabilities for the four outcomes (collisions, ejections, star grazers, and two planets) depend on the masses of both planets. However, based on a set of preliminary integrations, we found that the final orbital properties of the system within one of these outcome types depend on the ratio of planet masses, but are insensitive to the total planet mass. In Fig. 2, we illustrate this point by plotting the cumulative eccentricity distribution following an ejection for six sets of simulations each with a fixed mass (for both of the two planets). In light of the insensitivity to the total mass, we focused our n -body integrations of a series of seven sets of integrations with a constant total planet mass ratio, but varying $\beta \equiv m_{(2)}/(m_1 + m_2)$, where we use $m_{(1)}$ and $m_{(2)}$ to denote the mass of the more and less massive planets. In this set of integrations, we include an expanded range of planet masses ($10^{-4} \leq \mu_i < 10^{-2}$) and choose initial conditions that include both the more

massive planet having a smaller initial semi-major axis ($m_1 = m_{(1)}$) and the less massive planet having a smaller initial semi-major axis ($m_1 = m_{(2)}$). We choose a somewhat large total planet mass ratio, $\mu_1 + \mu_2 = 6 \times 10^{-3}$, so as to accelerate the evolution of the planetary systems and reduce the computational cost of the simulations.

3.2.1. Collisions

Collisions leave a single, larger planet in orbit around the star. Near the time of a collision, the energy in the center-of-mass frame of the two planets is much smaller than the gravitational binding energy of a giant planet to the star. Therefore, we model the collisions as completely inelastic and assume that the two giant planets simply merge together while conserving total momentum and mass. Using this assumption, the final orbit has a semi-major axis between the two initial semi-major axes, a small eccentricity, and a small inclination. In fact, we find that the final semi-major axis is only slightly less than would be estimated on the basis of energy conservation,

$$\frac{a_f}{a_1} \simeq \left[\frac{m_1}{m_1 + m_2} + \frac{m_2 a_1}{(m_1 + m_2) a_2} \right]^{-1}, \quad (1)$$

where a_f is the final semi-major axis of the remaining planet. This compares favorably with the results of our simulations and the magnitude of the deviations can be approximated (see appendix of FHR). We find that the fractions of our integrations that result in collisions decreases for more extreme planet mass ratios (assuming constant total planet mass). While collisions between planets may affect the masses of extrasolar planets, a single collision between two massive planets does not cause significant orbital migration or eccentricity growth if the planets are initially on low-eccentricity, low-inclination orbits near the Hill stability limit. Therefore, we shift our attention to those simulations that resulted in ejections.

3.2.2. Ejections

Since the escaping planet typically leaves the system with a very small (positive) energy (Moorehead & Adams 2005), energy conservation sets the final semimajor axis of the remaining planet slightly less than

$$\frac{a_f}{a_1} \simeq \left[\frac{m_1}{m_f} + \frac{a_1 m_2}{a_2 m_f} \right]^{-1} \quad (2)$$

Thus, the final semi-major axis of the planet left behind after an ejection depends on whether the more massive planet initially had the smaller or larger semi-major axis. Otherwise, the order of the planets makes little difference. Even in simulations with equal mass planets ($\beta = 0.5$), we find that the outer planet typically accounts for $\simeq 55\%$ of the ejections. When β is reduced only slightly to 0.45 or 0.40, then $\simeq 65\%$ or 80% of the ejections are of the less massive planet, regardless of which planet was initially closer. For $\beta \leq 0.30$, less than 1% of the ejections leave the less massive planet bound to the star. Therefore, we have combined the final eccentricities and inclinations of integrations with the same mass ratio, but reverse initial ordering of the planets. We present the mean and standard deviation of the final

planet's semi-major axis, eccentricity, and inclination for each set of simulations in Table 1 (based on a total of 6525 numerical integrations that resulted in one planet being ejected). Thus, the ejection of one of two equal-mass planets results in the most significant reduction in the semi-major axis, but is limited to $\frac{a_f}{a_{1,\text{init}}} \geq 0.5$.

In simulations resulting in an ejection, the remaining planet acquires a significant eccentricity, but its inclination typically remains small. The eccentricity and inclination distributions for the remaining planet are not sensitive to the sum of the planet masses, but depend significantly on the mass ratio. Both the final eccentricity and inclination are maximized for equal-mass planets.

In Fig. 3 we show the cumulative distributions for the eccentricity after an ejection for different mass ratios. While any one mass ratio results in a narrow range of eccentricities, a distribution of mass ratios would result in a broader distribution of final eccentricities. However, there is a maximum eccentricity, which occurs for equal-mass planets. Thus, the two-planet scattering model predicts that eccentricities rarely greater than $\simeq 0.8$, independent of the distribution of planet masses. We will compare this with the properties of known planets in § 4.

3.2.3. Stargazers

In a small fraction of our numerical integrations one planet underwent a close encounter with the central star (i.e., came within $10^{-2} \times a_{1,\text{init}}$). Note that the upper limit for the eccentricity of the remaining planet of 0.8 applies only after the other planet has been ejected from the system. Smaller pericenter separations can be achieved before a planet is ejected, while the orbits of both planets contain significant angular momentum. For our simulations with $\beta = 0.5$, $R_p/a_{1,\text{init}} = 10^{-4}$, $\simeq 3\%$ of all our integrations resulted in a star grazer. While the overall fraction of runs that result in stargazers is sensitive to the planetary radii, the ratio of the number of integrations that resulted in stargazers to the number that resulted in ejections is not. Additionally, the ratio of the number of integrations that resulted in stargazers to the number that resulted in ejections is likely to be less sensitive to our choice of initial conditions. For the same parameters, we find a ratio of $\simeq 0.06$. In our simulations with more extreme mass ratios, we find the total fraction of runs resulting in a star grazer is $\simeq 12\%$ or $\simeq 16\%$ for $\beta = 0.3$ or $\beta = 0.2$, and the ratio of star grazers to ejections is $\simeq 0.2$ or $\simeq 0.3$.

We must exercise caution in interpreting the above numbers. Due to the limitations of the numerical integrator used, the accuracy of our integrations for the subsequent evolution of systems resulting in star grazers cannot be guaranteed (Rauch & Holman 1999). Moreover, some of these planets could be directly accreted onto the star if their pericenters continue to decrease, or they might be ablated or destroyed by stellar winds/radiation (Vidal-Madjar et al. 2003, 2004; Murrar-Clay et al. 2005), or even ejected from the system following a strong tidal interaction (Faber, Rasio & Willems 2005). Moreover, the orbital dynamics of these systems might be affected by additional forces (e.g., tidal forces, interaction with the quadrupole moment of the star, general relativity; Adams & Laughlin 2006) that are not included in our simulations and would depend on the initial separa-

tion and the radius of the star. For example, Nagasawa et al. (2008) find that including tidal forces throughout the simulation can significantly increase the number of planets circularized in short-period orbits. Despite these complications, our simulations can provide constraints on the frequency of short-period planets formed via a combination of planet scattering and tidal dissipation.

The fraction of systems producing stargazers in our simulations is larger than the fraction of solar-type stars in radial velocity surveys that have very-hot-Jupiters ($1d \leq P \leq 3d$) or hot-Jupiters ($3d \leq P \leq 5d$), but smaller than the fraction of hot-Jupiters among detected extrasolar planets (Butler et al. 2006). The results of the OGLE-III transit search allow estimates for the frequency of hot-Jupiters ($\simeq (1_{-0.59}^{+1.39})/310$) and very-hot Jupiters ($\simeq (1_{-0.54}^{+1.10})/690$). Only the former rate is statistically consistent with current estimated rates based on radial velocity surveys ($\simeq 0.6\%$ for hot-Jupiters; Gould et al. 2006). While the fraction of solar-type stars with short-period giant planets is well constrained by existing radial velocity surveys, the frequency of long-period planets is not yet well constrained. The present detections provide a lower limit on their frequency, but this fraction is expected to increase as radial velocity surveys extend to longer temporal baselines. Improvements in measurement precision and instrument stability will enable the detection of less massive long-period planets, and is also likely to increase the number of long-period giant planets.

Given the limitations of our simulations and existing observations, it is most appropriate to compare: (a) the theoretical ratio of the number of systems (from our simulations) that resulted in stargazers to the number of systems that resulted in ejections to (b) the upper limit for the current observational ratio of the frequency of (very-)hot-Jupiters to the frequency of eccentric giant planets. Restricting our attention to planets with $m \sin i \geq 0.1 M_J$, we find 20 planets with orbital periods between 3 and 5 days (not including those recently discovered by the “N2K” project that focuses on short-period planets) and 80 planets with best-fit eccentricities greater than 0.2. Thus, we estimate the upper limit for the observational ratio to be $\simeq 20/80 = 0.25 \pm 0.06$. Given the uncertainties in both the observational and theoretical ratios, this suggests that planet-planet scattering could be responsible for a significant fraction of hot-Jupiters, if typical planetary systems form multiple giant planets. While radial velocity surveys are still incomplete, at least $\simeq 30\%$ of stars harboring one giant planet show evidence for additional distant giant planets (Wright et al. 2007). Thus, our simulations suggest that for giant planets with initial semimajor axes of a few AU, it is possible to achieve the extremely close pericenter distances necessary to initiate tidal circularization around a main sequence star and possibly leading to the formation of (very-)short-period planets (Rasio & Ford 1996; Rasio et al. 1996; Faber, Rasio & Willems 2005).

The planet scattering plus tidal circularization model for forming giant planets with very short orbital periods will be tested by future observations. Measurement of the Rossiter-McLaughlin effect could detect a significant relative inclination between the planet’s orbital angular momentum and the stellar rotation axis (Gaudi & Winn

2007) that could be induced by planet scattering (Chatterjee et al. 2008). Observations of $11^\circ \pm 15^\circ$ for HD 149026 (Wolf et al. 2007) and $30^\circ \pm 21^\circ$ for TrES-1 (Narita et al. 2007) are suggestive and will stimulate additional observations to improve the measurement precision. On the other hand, the detection of a Trojan companion to a short-period giant planet would suggest that the planet’s migration was less violent (e.g., Ford & Gaudi 2006; Ford & Holman 2007).

3.3. Final Semi-major Axes

The ejection of one of two giant planets results in an inward migration of the remaining planet, but this migration is limited by $\frac{a_f}{a_{1,\text{init}}} \geq 0.5$. Assuming that giant planets form (and emerge from the disk) at locations beyond the ice-line ($\sim 2.7\text{AU}$ for a solar mass star), two-planet scattering by itself is unlikely to explain the origins of giant planets with orbital periods $\ll 1.3\text{AU}$. However, the modest inward migration caused by two-planet scattering may be responsible for the observed increase in the frequency of giant planets at orbital periods just beyond ~ 1 year (and hence separations of $\sim 1\text{AU}$ for solar-type stars; Cumming et al. 2008).

A combination of planet scattering and tidal effects may be able to explain the origins of (very-)hot-Jupiters (§3.2.3; Nagasawa et al. 2008). However, the scattering of two giant planets has more difficulty explaining the presence of giant planets in nearly circular orbits at intermediate orbital periods $\sim 10\text{d} - 100\text{d}$, since their orbits are small enough to require significant migration, but large enough that tidal circularization is ineffective. Additional physics such as tidal effects and/or disk migration such planets may be necessary to explain such planets. For example, it might be possible to circularize such giant planets at intermediate distances, if the circularization occurs while the star is on the pre-main sequence and has a larger radius or while a sufficiently massive circumstellar disk is still present.

Of course intermediate-period planets may also have formed via some other mechanism (§1). For example, migration prior to instability could result in giant planets with these intermediate orbital period. In this case, the initial conditions of our simulations may not be representative, if two planets started with larger separations and the migration drove them into a mean motion resonance (e.g., 2:1 or 3:2). Therefore, more detailed simulations accounting for the planet-disk interactions are necessary to explore this scenario. For example, Adams & Laughlin (2003) explore pairs of migrating giant planets that typically become trapped in a 3:1 mean motion resonance, leading to eccentricity growth and eventually dynamical instability. Similarly, Moorhead & Adams (2005) consider planet scattering in the presence of type II migration and find that many systems evolve towards the 2:1 or 3:1 mean motion resonance. Both studies find that planet scattering plus planet-disk interactions are able to produce giant planets spread across a broad range of semi-major axes, including separations of less than $\sim 1\text{AU}$. However, these simulations do not produce a significant increase in the frequency of giant planets just beyond $\sim 1\text{AU}$, as inferred from radial velocity observations (Cumming et al. 2008). In any case, these simulations suggest that such planets can maintain large eccentricities

ties, despite the presence of eccentricity damping. While the detailed assumptions and initial conditions are different, it is noteworthy that both the idealized two-planet scattering experiments presented here and the simulations of Adams & Laughlin (2003) over-produce highly eccentric planets (relative to current observations; see §4.3).

4. COMPARISON WITH OBSERVATIONS

In this section, we investigate the observed distribution of eccentricities of extrasolar planets, based on the catalog of Butler et al. (2006), as updated by Johnson et al. (2006) and Wright et al. (2007). For comparing the observed eccentricity distribution to models, it is useful to exclude some of these planets, when the eccentricities are only weakly constrained by present observations. When the time span of radial velocity observations span less than two orbital periods, there can be significant degeneracies between the orbital period, eccentricity, and other parameters, and the bootstrap method of estimating uncertainties in orbital parameters can significantly underestimate the true uncertainties (Ford 2005). Therefore, we restrict our attention to planets with an orbital period less than half the time span of published radial velocity observations. Similarly, we exclude planets with orbital periods less than 10 days, since their eccentricities may have been altered due to tidal dissipation (Rasio et al. 1996). Of the 173 planets discovered by the radial velocity method, 136 meet both these criteria. Of these 136, the best-fit eccentricity for 86 planets exceeds 0.2. The abundance of giant planets with large eccentricities has led theorists to develop several models for exciting orbital eccentricities. Here we consider the implications of the observed eccentricity distribution for the planet-planet scattering model.

In order to test this, we compare the eccentricity distribution predicted by the two-planet scattering model to the observed eccentricity distribution.

We generated tens of thousands of new planetary systems containing two giant planets, assuming that the planet masses are uncorrelated. We assume that each of these systems would result in the less massive planet being ejected and estimate the final eccentricity of the more massive planet that remains bound. To determine the final eccentricity very efficiently, we use simple analytic fits to the mean and standard deviation of the eccentricity of the bound planet after one planet has been ejected, as a function of β , the planet mass ratio. We show the resulting eccentricity distributions in Fig. 4 for several different planet mass distributions. Within each panel, the different line styles indicate different choices of power-law index for the planet mass. These choices are based on a recent analysis of the Keck Planet Search estimated the mass-period distribution of giant planets with periods less than 2000 days. Cumming et al. (2008) found a best-fit mass power-law index of 0.31 ± 0.20 . Fig. 4 shows that in the two-planet scattering model, the final eccentricity following an ejection is relatively insensitive to this power law index (within the range consistent with observations). However, we find that the eccentricity distribution predicted by the two-planet scattering model is more sensitive to the choice for the lower cutoff of the planet-star mass ratio (μ_{lo}). If the typical planetary system forms two giant planets with masses dis-

tributed across two orders of magnitude ($\mu_{lo} = 10^{-4}$, $\mu_{hi} = 10^{-2}$), then the two-planet scattering model would over predict low eccentricity planets. On the other hand, if the typical planetary system forms two giant planets with masses distributed across only one orders of magnitude ($\mu_{lo} = 10^{-3}$, $\mu_{hi} = 10^{-2}$), then the two-planet scattering model would over-predict high eccentricity planets. For intermediate lower mass ratio cut-offs (e.g., $\mu_{lo} = 3 \times 10^{-3}$ or 5×10^{-4} , the predicted and observed eccentricity distributions show excellent agreement. Our results demonstrate that the exact distribution of eccentricities predicted will depend on the distribution of planet masses, including whether the masses of multiple planets that formed around one star are correlated. Understanding the distribution of planet masses and orbits is the subject of much ongoing research. Therefore, we first turn our attention to predictions of the planet scattering model that are insensitive to these uncertainties. In particular, the planet scattering model predicts that the planet that remains bound to the host star following an ejection will typically be the more massive of the two planets. As a result, the most extreme final eccentricities occur as the result of scattering of nearly equal mass planets. In the limiting case of equal mass planet scattering, the average final eccentricity was $\langle e_f \rangle = 0.624$ and the standard deviation was $\sigma_{e_f} = 0.135$. Therefore, the planet-planet scattering model predicts that eccentricities very rarely exceed $\simeq 0.8$. Then, we investigate what distribution of planet mass ratios would be necessary to explain the eccentricity distribution derived from present observations. Finally, we explore the potential for correlations between the eccentricity distribution and other properties to constrain theories for the origin of eccentricities, including the planet-planet scattering model.

4.1. Very High Eccentricity Planets

Of the 86 planets with orbital periods greater than 10 days and best-fit orbital eccentricities exceeding 0.2, two planets have eccentricities that are currently estimated to be greater than 0.8, HD 80606b ($e = 0.935 \pm 0.0023$; Naef et al. 2001) and HD 20782b ($e = 0.925 \pm 0.03$; Jones et al. 2006). Such large eccentricities are unlikely to be the result of planet-planet scattering (at least in the context of two planets initially on nearly circular orbits, as explored in §3.2.2). Thus, we search for alternative explanations for these two planets with extremely large eccentricities. First, we note that the eccentricity determination of HD 20782b is quite sensitive to a single night's observations. If the observations from that night are omitted, then the best-fit eccentricity would drop to 0.732, a value consistent with the planet-planet scattering model. Clearly, it would be desirable to obtain several additional radial velocity measurements around the time of future periastron passages to confirm the very large eccentricity.

Another possibility is that a wide stellar binary companion may have played a role in exciting such large eccentricities. Indeed, both of these planets orbit one member of a known stellar binary (Desidera & Barbieri 2007). For the sake of comparison, we note that only 19 out of the 86 planets in our sample orbit members of a known binary. In principle, secular perturbations due to a wide binary companion on an orbit with a large inclination relative to the planet's orbit can induce eccentricity os-

cillations with amplitudes approaching unity. However, the timescale for the eccentricity oscillations can be quite large for wide binaries, in which case other effects (e.g., general relativity or other planets) may lead to significant precession of the longitude of periastron and limit the amplitude of the eccentricity oscillations (Holman et al. 1997; Ford et al. 2000; Laughlin & Adams 2006; Takeda et al. 2008). For both HD 80606 and HD 20782, the orbit of the wide binary companion is unknown, limiting the utility of n-body integrations for these systems. Nevertheless, it is still possible to estimate the secular perturbation timescale based on the current projected separation of the binary companion. The current estimates in both of these systems are quite large (Desidera & Barbieri 2007). This has led to speculation that the “Kozai effect” may not be able to explain the large eccentricities for these two systems. The binarity may still be significant, e.g., if the two stars were not born as a binary, but rather the current binary companion originally orbited another star and was inserted into a wide orbit around the planetary system via an exchange interaction (a formation scenario similar to that proposed for the triple system PSR 1620–26; Ford et al. 2001; or other putative planets in multiple star systems; Portegies Zwart & McMillan 2005; Pfahl & Muterspaugh 2006; Malmberg et al. 2007b). During such an encounter, the four-body interactions might have induced a large eccentricity in the planetary orbit. Such interactions may have been common for stars born in clusters or other dense star forming regions (Adams & Laughlin 1998; Zakamska & Tremaine 2004).

We note that four other planets in our sample currently have a large best-fit eccentricity, but current observational uncertainties imply that they may or may not be a challenge to the planet-planet scattering model: HD 45450 ($e = 0.793 \pm 0.053$), HD 2039 (0.715 ± 0.046), HD 222582 ($e = 0.725 \pm 0.012$), and HD 187085 ($e = 0.75 \pm 0.1$). Additionally, some recently discovered planets—e.g., HD 137510 ($e = 0.359 \pm 0.028$) and HD 10647 ($e = 0.16 \pm 0.22$)—have modest best-fit eccentricities and formal uncertainty estimates, but a Bayesian analysis (following Ford et al. 2006) of the observations indicates significant parameter correlations and/or broad tails that still allow for very large eccentricities. We encourage observers to make additional observations of these known planetary systems, so as to improve the current observational uncertainties. Many observations spanning multiple periods with a high degree of long-term stability and good coverage near periastron passage are especially important for these particularly interesting high eccentricity systems that may provide insights into additional mechanisms for eccentricity excitation. We also encourage observers to pursue broad planet searches, so as to increase the number of known planets with very large eccentricities. Discovering a larger sample of such planets and follow-up observations help determine the role of binary companions in forming such systems.

4.2. Inferred Planet Mass Ratio Distribution

In §3, we demonstrated that the planet-planet scattering model predicts a large distribution of eccentricities and could account for 84 of 86 planets in the current sample. Thus, the planet-planet scattering model might be the dominant mechanism for exciting the eccentrici-

ties of extrasolar planets. In order to further explore this possibility, we consider the limiting case in which every planet’s eccentricity is presumed to be due to the planet having ejected exactly one other planet. Since the eccentricity of the remaining planet depends strongly on the mass ratio and the less massive planet is almost always ejected, we are able to transform the observed eccentricity distribution into a distribution of the inferred planet mass ratios (where $\beta_f = m_f/(m_1 + m_2)$ is the ratio of the mass of the putative ejected planet to the sum of masses of that planet and the remaining planet, assuming the orbits are coplanar). To perform this inversion, we assume that the final eccentricity is uniquely determined by the ratio of planet masses, and use the fitting formula $e_f = 1.44\beta_f^{1.23}$, based on the median eccentricities shown in Table 1 and Fig. 3. Since this fitting formula is based on the median eccentricities from our scattering simulations, it is expected that planet-planet scattering for equal-mass planets would result in some final eccentricities slightly greater than 0.62, the predicted median eccentricity evaluating our fitting formula at $\beta_f = 0.5$. Therefore our simple inversion of the fitting formula would result in β_f somewhat greater than 0.5 for some systems, even if the less massive planet had always been ejected.

To minimize contamination from either tidally circularized planets or planets with significant uncertainties in the orbital parameters, we again base our analysis on the eccentricities of extrasolar planets with orbital periods greater than 10 days, but less than half the time span of published radial velocity observations. We plot the cumulative distribution of β_f for this sample (Fig. 5, solid line), as well as a subset of these extrasolar planets where we have omitted planets in known binary systems (dotted line, 67 planets). For comparison, we consider the known multiple-planet systems and plot the cumulative distribution for β , the ratio of the second most massive planet to the sum of the masses of the two most massive (known) planets in the system (again assuming coplanarity; long dashed line). The distribution of inferred mass ratios is somewhat more extreme than the distribution of planet mass ratios for the known multiple planet systems. A two-sample Kolmogorov-Smirnov test yields a p -value of 0.19 or 0.14, including or excluding β ’s inferred from the current eccentricities of planets in known binaries. One possible explanation is that planetary systems with a timescale for instabilities that exceeds the current age of the star could have a different distribution of β than planetary systems that have already ejected a giant planet. Another possible explanation is that the typical history of a planetary system that currently contains a single giant planet might differ from the history of the typical planetary system that now has multiple giant planets. Despite these possibilities, we caution that any differences in the observed and inferred distributions of β and β_f may be due to observational selection effects. If a system has a small β , then one planet will typically have a much smaller velocity semi-amplitude and be more likely to have evaded detection.

As another point of reference, we show the cumulative distribution for β that would result from randomly choosing pairs of planets from our sample (which excludes planets with orbital periods less than 10 days or

longer than half the time span of published radial velocities, but includes planets in known binaries; short-dashed curve). We observe that this distribution is quite similar to the distribution of inferred β_f 's, differing only for $\beta \geq 0.45$. A two-sample Kolmogorov-Smirnov test yields a p -value of 0.21 or 0.06, depending on whether we include or exclude planets in known binary systems. In principle the difference might be due to nature rarely forming very nearly equal mass planets. However, we regard it as more likely that this difference is due to our assumptions that the less massive planet is always ejected and that the final eccentricity of the remaining planet is exactly determined by β (i.e., we ignore the dispersion of e_f observed in our scattering experiments). Clearly, this comparison is affected by the observational selection effects that favor detecting massive planets. Nevertheless, on the whole, this suggests that the planet scattering model can easily reproduce the observed eccentricity distribution (for planets with orbital periods greater than 10 d) by assuming a plausible mass distribution and no strong correlation between the masses of planets in multiple planet systems.

4.3. Observed Eccentricity Distribution

Next, we analyze the observed distribution of extrasolar planet eccentricities, without assuming that large eccentricities are due to planet scattering. As before, we restrict our attention to the extrasolar planets with orbital periods between 10 days and half the time span of published observations. We have performed a Bayesian analysis for each of the planets in the catalog of Butler et al. (2006), using the radial velocity data sets published by California and Carnegie Planet Search team. A detailed analysis will be presented separately, and here we only summarize our method. We assume the published model type (i.e., the number of planets and whether there is a long term trend) and apply the Markov chain Monte Carlo algorithm described in Ford (2005, 2006). Previous work has shown that the bootstrap-style estimates of parameter uncertainties employed by Butler et al. (2006) can differ significantly from uncertainty estimates based on the posterior probability distribution for model parameters (Ford 2005; Gregory 2005, 2006). Such differences are common for planets with eccentricities that are very near 0, planets with orbital periods comparable to the time span of observations, and planets with few and/or low signal-to-noise observations. Here, we focus our attention on the marginal posterior probability distributions for the orbital eccentricities. By restricting our attention to planets with orbital period greater than 10 days and less than half the timespan of observations, we obtain a sample for which the eccentricities are typically well-constrained by the observations and the two methods typically give qualitatively similar uncertainty estimates. We consider individually the multiple planet systems containing one or more planets with intermediate orbital periods and one planet with an orbital period likely longer than half the time span of observations. We determined that the uncertainty in the orbital parameters of the outer planet in the systems Hip 14810, HD 37124, and HD 190360 may significantly affect the orbital parameters of the other planets. Therefore, we dropped all planets in these systems from our sample.

To summarize the available information about the ec-

centricity distribution of extrasolar planets, we have averaged the marginal cumulative posterior eccentricity distribution for each planet in our sample (Figs. 6 & 7, dotted curve, all panels) for the sample including and excluding planets orbiting known binary stars.

It is important to note that this method does not provide a Bayesian estimate of the eccentricity distribution of the population. Instead, these summary distributions can be intuitively thought of as a generalization of the classical histogram that accounts for the uncertainties in the individual eccentricities in a Bayesian way (allowing for non-Gaussian posterior distributions). However, like classical histograms, our summary distributions can be affected by biases (e.g., the terminal age bias for dating field stars with stellar models; Pont & Eyer 2004; Takeda et al. 2006). While we have attempted to minimize the potential influence of any systematic biases (by selecting a subset of extrasolar planets for which the eccentricities were well constrained by observational data), our summary distributions are still influenced by the shape of individual posterior distributions. Performing a proper Bayesian population analysis would require more sophisticated and much more computationally demanding calculations (e.g., Ford & Rasio 2006). Nevertheless, we believe that these distributions can serve as a valuable summary of the available information about the eccentricity distribution of extrasolar planets.

For the sake of comparison, we present similar summary information for the observed eccentricity distribution based on the orbital determinations of Butler et al. (2006). For this purpose, we approximate each planet's marginal cumulative eccentricity distribution as

$$p(e) = \frac{\text{erf}((e - e_{\text{bf}})/\sigma_e) - \text{erf}(-e_{\text{bf}}/\sigma_e)}{\text{erf}((1 - e_{\text{bf}})/\sigma_e) - \text{erf}(-e_{\text{bf}}/\sigma_e)}, \quad (3)$$

where e_{bf} is the best fit eccentricity and σ_e is the uncertainty in the eccentricity, both taken from Butler et al. (2006). The results are presented in Figures 6a and 7b, dashed curve) for the sample including and excluding planets orbiting known binary stars. The strong similarity of these two distributions demonstrates that this distribution is well determined and that this can be used as a robust summary of the observed planet eccentricities.

4.3.1. Does the Eccentricity Distribution Vary with Planet Mass?

Next, we investigate whether the eccentricity distribution is correlated with other planet properties. Such differences have the potential to provide insights into the processes of planet formation. For example, Black (1997) and Stepinsky & Black (2000) noted similarities in the period-eccentricity distributions of extrasolar planets and binary stars, and suggested that both sets of objects may in fact be one extended population. More recent work identified differences in the two distributions and favors the hypothesis that these two populations have different formation mechanisms (Halbwachet, Mayor & Udry 20005).

Most recently, Ribas & Miralda-Escude (2006) noted a potential correlation between a planet's mass and its orbital eccentricity. They propose that this could be due to two different formation mechanisms, e.g., core accretion followed by gas accretion dominating the formation

of planets with $m \sin i \leq 4M_J$ and direct collapse of gas from the protoplanetary nebulae dominating the formation of planets with $m \sin i \leq 4M_J$. Ribas & Miralda-Escude (2006) divided their sample according to $m \sin i$ being greater than or less than $4M_J$, and test the null hypothesis that the two samples came from the same distribution using the two sample Kolmogorov-Smirnov test. Their choice of $4M_J$ was based on the claimed separation of exoplanets into two populations based on apparent planet mass-stellar metallicity correlation. Since this distinction is only marginal, we worry that their choice of $4M_J$, we caution against over-interpretation of their p -values that can occur due to *a posteriori* statistical analyses.

We explore this hypothesis by comparing the eccentricity distributions of various subsets of the extrasolar planet population (presented in aggregate as the dotted curve in each panel of Fig. 6 & 7). First, we divide the planet sample according to the best-fit $m \sin i$ (Fig. 6b). In order to avoid complications associated with *a posteriori* statistics, we choose to perform a single statistical test, dividing our sample into two nearly equal sized subsamples (they differ in sample size by one): $m \sin i \leq 1.57M_J$ (dashed curve) and $m \sin i > 1.57M_J$ (solid curve). Similar eccentricity distributions that do not include any planets in known binary systems are presented in Fig. 7b. The same choices of mass ranges results in subsample sizes that differ by at most three. A two-sample Kolmogorov-Smirnov test results in p -values of 0.024 and 0.093 for the samples including and excluding planets in binaries. (If we had instead divided our sample at $m \sin i = 4M_J$, we would have obtained p -values of 0.004 and 0.023.) By analyzing planets in systems with no known binary companion, we minimize the potential for eccentricity excitation by a stellar binary. Since the K-S test only suggests a marginally significant difference between the high- and low-mass planets orbiting stars with no known binary companion, we conclude that a larger sample of extrasolar planets is necessary to test this hypothesis.

The sign of any putative correlation between planet mass and eccentricity is also notable. It is the more massive planets that are claimed to be more eccentric. Many models of eccentricity excitation would predict that it is easier to increase the eccentricity of lower-mass planets, since a larger torque is required to excite the eccentricity of a more massive planet. One possible explanation is that most planetary systems produce eccentric giant planets, but the amount of subsequent eccentricity damping varies from one system to another. If the late stage eccentricity damping is determined by the mass of the planetesimal disk relative to the planet mass, then this model could explain the larger eccentricities of more massive planets. Further, the large dispersion in the time until the onset of dynamical instability would result in a large dispersion in the amount of eccentricity damping after the most recent strong planet scattering event, and thus provide a natural mechanism for explaining both the small eccentricities of the planets in the solar system and the large eccentricities of extrasolar giant planets. Furthermore, this scenario would predict that more massive planets would tend to have larger eccentricities.

4.3.2. Does the Eccentricity Distribution Vary with Orbital Period?

Next, we present a similar analysis, but dividing our planet sample according to the best-fit orbital period (Figs. 6c & 7c), rather than $m \sin i$. A difference in these distributions might be expected if eccentricity excitation is strongly correlated with planet migration (Artymowicz 1992; Papaloizou & Larwood 2000; Papaloizou & Terquem 2001; Goldreich & Sari 2003; Ogilvie & Lubow 2003; Cresswell & Nelson 2007). If we assume that giant planets form at large distances and migrate inwards, then planets that are currently have smaller semi-major axes would be expected to have experience more migration. To test this hypothesis, we divide our sample into two subsets: $P > 350\text{days}$ (solid curve) and $P < 350\text{days}$ (dashed curve). Again, the boundary between the two subsamples is chosen so that size of the two sub samples are equal or differ by only one when we include binaries and three when we exclude binaries. Clearly, the distributions are quite similar. Formally, a two sample K-S test results in p -values of 0.87 and 0.96 for the samples that include and exclude planets in binary systems. Thus, we conclude that the current planet sample contains no significant differences in the eccentricity distributions of planets with orbital periods of $10\text{d} \leq P \leq 330\text{d}$ and those with $330\text{d} \leq P \leq T_{\text{obs}}/2$, and we find no observational support for eccentricity excitation via migration.

It is natural to ask if the large torques presumed responsible for orbital migration could also be responsible for exciting orbital eccentricities. While the dissipative nature of a gaseous disk naturally leads to eccentricity damping (Artymowicz 1993), a few researchers have suggested that excitation may also be possible. Artymowicz (1992) found that a sufficiently massive giant planet ($\geq 10 M_{\text{Jup}}$) can open a wide gap, leading to torques which excite eccentricities. More recently, Goldreich & Sari (2003) have suggested that a gas disk could excite eccentricities even for less massive planets via a finite amplitude instability. This claim is controversial, as 3-d numerical simulations have not been able to reproduce this behavior (e.g., Papalouizou et al. 2001; Ogilvie & Lubow 2003; Moorhead & Adams 2008). Given the large dynamic ranges involved and the complexity of the simulations, one might question the accuracy of current simulations. For example, 3-d simulations have suggested that the gaps induced by giant planets might not be as well cleared as assumed in many 2-d disk models (Bate et al. 2003; D'Angelo et al. 2003). We believe that further theoretical and numerical work is needed to better understand planet-disk interactions. In the meantime, we look to the observations for guidance on the question of eccentricity damping or excitation.

In the GJ876 system, the observed eccentricities are not consistent with eccentricity excitation via interactions with the disk. The current observed eccentricities could be readily explained if interactions with a gas disk led to strong eccentricity damping $K = \dot{e}a/\dot{e}a \gg 1$ (Lee & Peale 2002; Kley et al. 2005). This is in sharp contrast to current hydrodynamic simulations of migration that suggest $K \simeq 1$ and theories that predict $K < 0$ (e.g., Goldreich & Sari 2003; Ogilvie & Lubow 2003). While other resonant planetary systems are not yet as well con-

strained or studied as GJ 876, the moderate eccentricities of other extrasolar planetary systems near the 2:1 mean motion resonance suggest that GJ 876 is not unique.

The ν And system also provides a constraint on eccentricity excitation during migration. If the outer two planets migrated to their current locations (0.8 and 2.5 AU), then they must have been in nearly circular orbits at the time of the impulsive perturbation in order for the middle planet's eccentricity to periodically return to nearly zero (Ford et al. 2005). While this does not demonstrate a need for rapid eccentricity damping as in GJ 876, it is inconsistent with models that predict significant eccentricity excitation. Since dynamical analyses severely limit the possibility of eccentricity excitation in both the GJ 876 and ν And systems, we conclude that orbital migration does not typically excite eccentricities, at least for a planet-star mass ratio less than $\sim 0.003 - 0.006$ (those of the most massive planet in ν And and GJ 876).

4.3.3. Does the Eccentricity Distribution Vary with the Ability of the Planet to Eject Lower-Mass Objects?

The next investigation is motivated by theoretical models for eccentricity excitation via planet-planet scattering and the dynamical relaxation of packed planetary systems (see §1 and references therein). Migration due to scattering of a planetesimal disk might also result in eccentricity growth for very massive giant planets, $m_p/M \geq 0.01$; Murray et al. 1998). In each of these models, close encounters can result in either two bodies colliding (resulting in a more massive planet, but not significant eccentricity growth) or one body being ejected (resulting in eccentricity growth for the remaining planet). The frequency of these two outcomes depends on

$$\theta^2 \equiv \left(\frac{Gm}{R_p} \right) \left(\frac{r}{GM_\star} \right) \quad (4)$$

$$= 10 \left(\frac{m}{M_J} \right) \left(\frac{M_\odot}{M_\star} \right) \left(\frac{R_J}{R_p} \right) \left(\frac{r}{5 \text{ AU}} \right), \quad (5)$$

where R_p is the radius of the planet (or the effective radius for collision), r is the distance separating the star from the planet at the time of the close encounter. Since we do not know the exact distance for r , we set it equal to the current apastron distance of the observed planet, $a(1+e)$. When $\theta \gg 1$, the planet is able to efficiently eject bodies, but when $\theta < 1$, collisions will be much more frequent.

We investigate whether the eccentricity distribution is correlated with θ , by dividing the planet sample according to the ratio of the escape velocity from the planet (evaluated at the surface of the planet) to the escape velocity from the star (evaluated at the apastron distance of the planet) in Figures 6d and 7d. Since radial velocity observations measure $m \sin i$, we compare two subsamples with $\theta^2 \sin i \geq 1.69$ (solid line) and $\theta^2 \sin i < 1.69$ (dashed line). Again, the samples are divided such that the equal numbers of planets in each subsample differs by only one. Since planets with large θ eject other bodies more efficiently, the planet scattering model predicts that massive planets are more likely to acquire large eccentricities. This expectation is consistent with the sign of any putative correlation between the planet eccentricity and θ seen in Figures 6d and 7d. A two-sample K-S test results in p -values of 0.020 and 0.100 for samples

that include or exclude planets in known binary systems. Thus, we find that the putative dependence of the eccentricity distribution on θ is essentially just as statistically significant as the suggested dependence on planet mass (Butler et al. 2006; Ribas & Miralda-Escude 2006). Nevertheless, we caution that both putative correlations are at most marginally significant at this time. More importantly, the similar statistical significance of two putative correlations of the eccentricity distribution with the planet mass or θ demonstrate that even when one model correctly predicts a correlation, other models may make similar predictions. Thus, it is important that theorists explore the implications of a broad range of theoretical models and observers provide observations that can test each of these predictions.

We conclude that a larger sample of extrasolar planets would be valuable for testing hypotheses about the origins of large eccentricities. The current sample of $\simeq 200$ extrasolar planets, has allowed several particularly interesting systems to provide valuable constraints on planet formation and eccentricity excitation. Additionally, the current sample is suitable for identifying (or refuting) strong correlations, such as the planet frequency-stellar metallicity correlation (Fisher & Valenti 2005). However, many other statistical analyses of the extrasolar planet population will require the discovery of many more extrasolar planets. While transit searches have the potential to discover many additional extrasolar giant planets in the coming years, ground-based transit surveys will be strongly biased towards short-period planets for which tidal dissipation is likely to have circularized their orbits (Rasio et al. 1996). These will certainly be quite valuable for testing theories of planet migration (e.g., Ford & Rasio 2006) and planetary structure (e.g., Bodenheimer, Laughlin & Lin 2003). However, statistical investigations of eccentricity excitation mechanisms will require discoveries many planets with intermediate to long-period orbits. Thus, we encourage observers to apply other planet search techniques to large samples (e.g., “N2K” project; Fischer et al. 2004). Fortunately, the CoRoT and Kepler space missions will be able to detect transiting planets with larger separations where tidal circularization is not significant. It will be particularly interesting to study the eccentricities of any rocky transiting planets found by CoRoT and Kepler. While it will be extremely challenging to measure the eccentricity of distant rocky planets via the radial velocity method, it will be possible to characterize the eccentricity distribution of such planets (in a statistical sense) even without radial velocity observations (Ford et al. 2008).

4.4. Could Binaries and Planet Scattering Explain all Large Eccentricities?

Both secular perturbations from a binary companion and planet-planet scattering appear very likely to play a significant role in exciting the eccentricities of extrasolar planets, but it is not clear if additional mechanisms commonly excite eccentricities. Therefore, we searched through the catalog of known extrasolar planets to identify those with large eccentricities that appear unlikely to be due to either secular perturbations from a wide binary companion or planet scattering. We summarize this information in Fig. 8. Of the 173 radial velocity planets, 89 have best-fit eccentricities greater than 0.2.

Of those 89, 23 have a known binary companion and 74 have $\theta \sin i > 1$. This leaves 11 eccentric planets for which the eccentricity cannot be explained by secular perturbations by a known wide binary companion or by planet–planet scattering involving that planet. In three of these cases, the eccentricity may still have been excited by the perturbation from another giant planet in the system. We discuss each of these briefly. HD 74156 hosts a second planet that is both eccentric and capable of ejecting other objects ($\theta^2 \sin i \simeq 25$). Radial velocities of HD 118203 reveal a long-term trend that is likely to be due to a second more distant giant companion. While the orbit is highly uncertain, the slope and time-span of observations suggest that the putative second planet is most likely to be more massive than HD 118203b and have a semi-major axis of at least 1.7 AU. If true, then the putative distant giant planet would be able to eject other objects and excite an eccentricity in HD 118203b. Alternatively, the best-fit eccentricity may be an artifact due to the radial velocity perturbations of one or more additional planets. Observations also show a long-term trend in HD 49674. While the magnitude is smaller, the longer time span of radial velocity observations imply that the putative planet most likely has an orbital period beyond 5 AU, so it too is likely able to eject other objects. GJ 876 contains three planets and the outer two are participating in a 2:1 mean motion resonances. Detailed modeling of this system suggests that the eccentricities of both GJ 876b and GJ 876c are likely due to eccentricity excitation that occurred due to convergent migration and resonance capture (Lee & Peale 2002; Kley et al. 2004). Technically, GJ 876c is massive enough to eject other bodies ($\theta^2 \sin i \simeq 1.2$), so a hybrid scenario of planet scattering and resonant capture is possible (e.g., Sandor & Kley 2006).

This leaves 7 out of 89 eccentric planets that cannot be explained by secular perturbations from a known wide binary or by planet–planet scattering by any planet which is currently supported with radial velocity observations (HD 33283b, HD 108147b, HD 117618b, HD 208487b, HD 216770b, Hip 14810c), unless $\sin i \ll 1$. Of course, these systems may have an undetected binary companion. For example, there is preliminary evidence for a binary companion to HD 52265 (Chauvin et al. 2006), but follow-up observations are needed to confirm this. Similarly, there may be additional undetected planets. We note that over half of these systems were discovered only in the last two years, most have a relatively modest number of radial velocity observations, and over half of these have a relatively modest signal-to-noise ratio (velocity semi-amplitude over the effective single measurement precision).

Thus, there is a very real possibility that additional radial velocity observations may result in revisions to the measured eccentricity (e.g., GJ 436b), the detection of a long-term trend most likely due to a distant giant planet, and/or the detection of additional planets. The uncertainties in the orbital elements can be particularly problematic in cases where there is an undetected planet is near a 2:1 or 3:1 mean motion resonance. Previous experience has taught that the perturbations from yet undetected planets can lead to significant overestimates of the eccentricity. We encourage additional observations of

these systems, which may prove particularly interesting for testing theories of eccentricity excitation. We note that HD 108147, Hip 14810, HD 33283, HD 52265, and HD 216770 are particularly favorable, since they have velocity amplitudes and eccentricities such that one eccentric planet could be differentiated from two planets in a mean motion resonance. We will present a more detailed discussion of resonant systems in a future paper. If future observations were to confirm the sizable eccentricity, the lack of other massive companions (both giant planet and stellar companions), then these systems would provide evidence for at least one additional eccentricity excitation mechanism in addition to planet–planet scattering, secular perturbations from binaries, and resonant capture.

5. CONCLUSIONS

A planetary system with two or more giant planets may become dynamically unstable, leading to a collision or the ejection of one of the planets from the system. Early simulations for equal-mass planets revealed discrepancies between the results of numerical simulations and the observed orbital elements of extrasolar planets. However, our new simulations for two planets with *unequal masses* show a reduced frequency of collisions as compared to scattering between equal-mass planets and suggest that the two-planet scattering model can reproduce the observed eccentricities with a plausible distribution of planet mass ratios.

Additionally, the two-planet scattering model predicts a maximum eccentricity of ~ 0.8 , which is independent of the distribution of planet mass ratios. This predicted eccentricity limit compares favorably with current observations and will be tested by future planet discoveries. The current sample of extrasolar planets provides hints of a correlation between the eccentricity distribution and other properties. We show that the putative correlation between eccentricity distribution and the ratio of the escape velocity from the planet to the escape velocity from the star is comparable in statistical significance to the putative correlation between the eccentricity distribution and planet mass. Additionally, both correlations remain marginally significant, when we exclude planets in known binary systems. We have identified a few particularly interesting planets that are unlikely to be explained by the two-planet scattering model, since $\theta^2 \sin i < 1$. We encourage additional observations of these systems to determine if these are isolated planets or if there may be other planets in the system that could excite large eccentricities and/or cause the current eccentricity to be overestimated.

The combination of planet–planet scattering and tidal circularization may be able to explain the existence of giant planets in very short period orbits. However, the presence of giant planets at slightly larger orbital periods (small enough to require significant migration, but large enough that tidal circularization is ineffective) is more difficult to explain. Finally, the planet–planet scattering model predicts a significant number of extremely loosely bound and free floating giant planets, which may also be observable (Lucas & Roche 2000; Zapatero Osorio et al. 2002; Veras et al. in prep).

A complete theory of planet formation must explain both the eccentric orbits prevalent among extrasolar

planets and the nearly circular orbits in the Solar System. Despite significant uncertainties about giant planet formation, the leading models for the formation and early dynamical evolution of the Solar System's giant planets agree that the giant planets in the Solar System went through a phase of large eccentricities (Levison et al. 1998; Thommes et al. 1999, 2002; Tsiganis et al. 2005; Ford & Chaing 2007). If Uranus and Neptune formed closer to the Sun, then close encounters are necessary to scatter them outwards to their current orbital distances. During this phase, their eccentricities can exceed $\simeq 0.5$ (Tsiganis et al. 2005). Alternatively, if Uranus and Neptune were able to form near their current locations, then oligarch growth predicts that several other ice giants should have formed contemporaneously in the region between Uranus and Neptune (Goldreich, Lithwick & Sari 2004). The scattering necessary to remove these extra ice giants would have excited sizable eccentricities in Uranus and Neptune (Ford & Chaing 2007; Levison & Morbidelli 2007). Finally, the gravitational instability model predicts that most giant planets form with significant eccentricities (Boss 1995). Therefore, it seems most likely that even the giant planets in our Solar System were once eccentric.

Perhaps the question, "What mechanism excites the eccentricity of extrasolar planets?" should be replaced with "What mechanism damps the eccentricities of giant planets?" Unless giant planets form via gravitational instability, interactions with a gas disk are not an option, since the eccentricities would have been excited after the gas was cleared. Both dynamical friction within a planetesimal disk and planetesimal scattering could damp eccentricities in both the Solar System and other planetary systems. Dynamical friction alone would not clear the small bodies, so either accretion or ejection would be required to satisfy observational constraints (Goldreich, Lithwick & Sari 2004). Planetesimal scattering provides

a natural mechanism to simultaneously damp eccentricities and remove small bodies from planetary systems.

Perhaps, *the key parameter that determines whether a planetary system will have eccentric or nearly circular orbits is the amount of mass in planetesimals at the time of the last strong planet-planet scattering event.* This could explain why more massive planets may tend to have larger eccentricities. Additionally, the chaotic evolution of multiple planet systems naturally provides a large dispersion in the time until dynamical instability results in close encounters (Chambers, Wetherill & Boss 1996; FHR; Marzari & Weidenschilling 2002; Chatterjee et al. 2008). This could explain why some planetary systems have large eccentricities (late stage instability when there was little disk to damp eccentricities), while our planets in the Solar System have nearly circular orbits (last instability occurred while sufficient planetesimal disk to damp eccentricities). Unfortunately, this model would significantly complicate the interpretation of the observed eccentricity distribution for some extrasolar planets. Investigations of dynamical instabilities in systems with three or more planets have only begun to explore the large available parameter space. Future numerical investigations will be necessary to test such theoretical models.

We thank E.I. Chiang, M. Holman, G. Laughlin, M.H. Lee, H. Levison, G.W. Marcy, A. Morbidelli, J.C.B. Papaloizou, S. Peale, and J. Wright for useful discussions and the anonymous referee for a thoughtful review. Support for E.B.F. was provided by the University of Florida, a Miller Research Fellowship and by NASA through Hubble Fellowship grant HST-HF-01195.01A awarded by the Space Telescope Science Institute, which is operated by the Association of Universities for Research in Astronomy, Inc., for NASA, under contract NAS 5-26555. This work was supported by NSF grants AST-0206182 and AST-0507727 at Northwestern University.

REFERENCES

- Adams, F. C., & Laughlin, G. 2003, *Icarus*, 163, 290
 Adams, F. C., & Laughlin, G. 2006, *ApJ*, 649, 1004
 Alexander, R. D., Clarke, C. J., & Pringle, J. E. 2006, *MNRAS*, 369, 229
 Artymowicz 1992 *PASP* 104, 769.
 Artymowicz 1993 *ApJ* 419, 116.
 Barnes, R., & Greenberg, R. 2006, *ApJ*, 638, 478
 Barnes, R., & Greenberg, R. 2006, *ApJ*, 647, L163
 Barnes, R. Qunn, T. 2004 *ApJ* 611, 494.
 Bate, M.R., Lubow, S.H., Ogilvie, G.I., Miller, K.A. 2003 *MNRAS* 341, 213.
 Black, D. C. 1997, *ApJ*, 490, L171
 Bodenheimer, P., Laughlin, G., & Lin, D. N. C. 2003, *ApJ*, 592, 555
 Boss, A.P. 1995 *Science*, 267, 360.
 Butler, R. P., et al. 2006, *ApJ*, 646, 505
 Chambers, J. E. 1999, *MNRAS*, 304, 793
 Chambers, J.E., Wetherill, G.W. & Boss, A.P. 1996 *Icarus* 119, 261.
 Chatterjee, S., Ford, E.B., Rasio, F.A. 2008, *ApJ*, in press. [[arxiv:astro-ph/0703166](https://arxiv.org/abs/astro-ph/0703166)]
 Chauvin, G., Lagrange, A.-M., Udry, S., Fusco, T., Galland, F., Naef, D., Beuzit, J.-L., & Mayor, M. 2006, *A&A*, 456, 1165
 Chiang, E.I. 2003 *ApJ* 584, 465.
 Chiang, E.I. & Murray, N. 2002 *ApJ* 576, 473.
 Cresswell, P., Dirksen, G., Kley, W., & Nelson, R. P. 2007, *A&A*, 473, 329
 Cumming, A., Butler, R. P., Marcy, G. W., Vogt, S. S., Wright, J. T., & Fischer, D. A. 2008, *PASP* 120, 531.
 D'Angelo, G., Kley, W., Henning, T. 2003 *ApJ* 586, 540.
 Desidera, S., & Barbieri, M. 2007, *A&A*, 462, 1039.
 Faber, J.A., Rasio, F.A. & Willems, B. 2005 *Icarus*, 175, 248
 Fischer, D. A., et al. 2005, *ApJ*, 620, 481
 Ford, E. B. 2005, *AJ*, 129, 1706
 Ford, E. B. 2006, *ApJ*, 642, 505 *Orbits of Extrasolar Planets*
 Ford, E.B. & Chaing, E.I. 2007, *ApJ*, 661, 602.
 Ford, E.B. & Gaudi, B.S. 2006, *ApJ*, 652, L137.
 Ford, E.B., Havlickova, M. & Rasio, F.A. 2001 *Icarus* 150, 303.
 Ford, E.B. & Holman, M. 2007, *ApJL* 664, 51.
 Ford, E.B., Kozinsky, B., Rasio, F.A. 2000 *ApJ* 535, 385.
 Ford, E.B., Lystad, V., Rasio, F.A. 2005 *Nature* 434, 873.
 Ford, E. B., Quinn, S. N., & Veras, D. 2008, *ApJ*, in press. [[arXiv:0801.2591](https://arxiv.org/abs/0801.2591)]
 Ford, E.B. & Rasio, F.A. 2006, *ApJ*, 638, L45.
 Ford, E.B., Rasio, F.A., Yu, K. 2003 *Scientific Frontiers in Research on Extrasolar Planets*, eds. D. Deming & S. Seager (ASP Conference Series, 294), 181.
 Gaudi, B.S. & Winn, J.N. 2007, *ApJ* 655, 550.
 Gladman, B. 1993 *Icarus*, 106, 247.
 Goldreich, P., Lithwick, Y., Sari, R. 2004 *ApJ* 614, 497.
 Goldreich, P., Sari, R. 2003 *ApJ* 585, 1024.
 Goldreich, P., Tremaine, S. 1979 *ApJ* 233, 857.
 Goldreich, P., Tremaine, S. 1980 *ApJ* 241, 425.
 Gregory, P. C. 2005, *ApJ*, 631, 1198
 Gregory, P. C. 2006, *MNRAS*, 1375
 Halbwachs, J.L., Mayor, M., Udry, S. 2005 *A&A* 431, 1129.
 Holman, M., Touma, J., Tremaine, S. 1997 *Nature* 386, 254.
 Hurley, J. R., & Shara, M. M. 2002, *ApJ*, 565, 1251

- Johnson, J. A., et al. 2006, *ApJ*, 647, 600
- Jones, H. R. A., Butler, R. P., Tinney, C. G., Marcy, G. W., Carter, B. D., Penny, A. J., McCarthy, C., & Bailey, J. 2006, *MNRAS*, 369, 249
- Juric, M. & Tremaine, S. 2008, *ApJ*, in press. [arxiv:astro-ph/0703160]
- Kley, W. 2000 *MNRAS* 313, L47.
- Kley, W., Lee, M.H., Murray, N., Peale, S.J. 2005 *A&A* 437, 727.
- Kley, W., Peitz, J. & Bryden, G. 2004 *A&A*, 414, 735.
- Kley, W., Lee, M. H., Murray, N., & Peale, S. J. 2005, *A&A*, 437, 727
- Kokubo, E. & Ida, S. 1998a *Icarus* 123, 180.
- Kokubo, E. & Ida, S. 1998b *Icarus* 131, 171.
- Laughlin, G., & Adams, F. C. 1998, *ApJ*, 508, L171
- Lee, M.H. & Peale, S.J. 2002 *ApJ* 567, 596.
- Lee, M.H. & Peale, S.J. 2003 *ApJ* 592, 1201.
- Lee, A. T., Thommes, E. W., & Rasio, F. A. 2008, *ArXiv e-prints*, 801, arXiv:0801.1926
- Levison, H.F., Lissauer, J.J., Duncan, M.J. 1998 *AJ* 116, 1998.
- Lin, D.N.C. & Ida, S. 1997 *ApJ*, 447, 781
- Lissauer, J.J. 1993 *ARAA*, 31, 129
- Lissauer, J.J. 1995 *Icarus* 114, 217.
- Malmberg, D., Davies, M. B., & Chambers, J. E. 2007a, *MNRAS*, 377, L1
- Malmberg, D., de Angeli, F., Davies, M. B., Church, R. P., Mackey, D., & Wilkinson, M. I. 2007b, *MNRAS*, 378, 1207
- Marzari, F., & Weidenschilling, S. J. 2002, *Icarus*, 156, 570
- Marzari, F., Weidenschilling, S. J., Barbieri, M., & Granata, V. 2005, *ApJ*, 618, 502
- Mazeh, T., Krymowski, Y., Rosenfield, G. 1997, *ApJ*, 447, L103.
- Moorhead, A. V., & Adams, F. C. 2005, *Icarus*, 178, 517
- Moorhead, A. V., & Adams, F. C. 2008, *Icarus*, 193, 475
- Murray, N. Hansen, B., Holman, M., Tremaine, S. 1998 *Science* 279, 69.
- Naef, D., et al. 2001, *A&A*, 375, L27
- Nagasawa, M., Lin, D.N.C., Ida, S. 2003 *ApJ* 586, 1374.
- Nagasawa, M., Ida, S., Bessho, T. 2008, *ApJ*, 678, 498.
- Namouni, F., & Zhou, J. L. 2006, *Celestial Mechanics and Dynamical Astronomy*, 95, 245
- Namouni, F. 2005, *AJ*, 130, 280
- Narita, N. et al. 2007 *PASJ*, 60, L1.
- Ogilvie & Lubow 2003 *ApJ* 587, 398.
- Papaloizou, J. C. B., & Larwood, J. D. 2000, *MNRAS*, 315, 823
- Papaloizou, J.C.B. & Terquem, C. 2001 *MNRAS* 325, 221.
- Papaloizou, J.C.B. & Terquem, C. 2002 *MNRAS* 332, L39.
- Papalouizou, J.C.B., Nelson, R.P. & Masset, F. 2001 *A&A* 366, 263.
- Pfahl, E. & Mutterspaugh, M. 2006 *ApJ*, 652, 1694.
- Pollack, J.B., Hubickyj, O., Bodenheimer, P., Lissauer, J.J., Podolak, M. & Greenzweig, Y. 1996 *Icarus* 124, 62.
- Pont, F., & Eyer, L. 2004, *MNRAS*, 351, 487
- Portegies Zwart, S.F. & McMillan, S.L.W. 2005 *ApJ* 633, 141.
- Rasio, F.A. & Ford, E.B. 1996 *Science* 274, 954.
- Rasio, F.A., Tout, C.A., Lubow, S.H. & Livio, M. 1996 *ApJ*, 470, 1187.
- Rauch, K. P., & Holman, M. 1999, *AJ*, 117, 1087
- Ribas, I., & Miralda-Escude, J. 2007, *A&A* 464, 779.
- Sándor, Z., & Kley, W. 2006, *A&A*, 451, L31
- Schäfer, C., Speith, R., Hipp, M., & Kley, W. 2004, *A&A*, 418, 325
- Stepinsky, T.F. & Black, D.C. 2000, *A&A*, 356, 903
- Stepinsky, T.F., Malhotra, R., & Black, D.C. 2000 *ApJ* 545, 1004.
- Takeda, G., Kita, R., & Rasio, F. A. 2008, submitted to *ApJ*, ArXiv e-prints, 802, arXiv:0802.4088
- Takeda, G., & Rasio, F. A. 2005, *ApJ*, 627, 1001
- Takeda, G., & Rasio, F. A. 2006, *Ap&SS*, 19
- Thommes, E. W., Duncan, M. J., & Levison, H. F. 1999, *Nature*, 402, 635
- Thommes, E. W., Duncan, M. J., & Levison, H. F. 2002, *AJ*, 123, 2862
- Trilling, D. E., Benz, W., Guillot, T., Lunine, J. I., Hubbard, W. B., & Burrows, A. 1998, *ApJ*, 500, 428
- Tsiganis, K., Gomes, R., Morbidelli, A., Levison, H.F. 2005 *Nature* 435, 459.
- Veras, D. Armitage, P.J. 2004 *Icarus* 172, 349.
- Veras, D. Armitage, P.J. 2005 *ApJ*, 620, L111.
- Veras, D. Armitage, P.J. 2006 *ApJ*, 645, 1509.
- Vidal-Madjar, A., Lecavelier des Etangs, A., Désert, J.-M., Ballester, G. E., Ferlet, R., Hébrard, G., & Mayor, M. 2003, *Nature*, 422, 143
- Weidenschillingm S.J. & Marzari, F. 1996 *Nature* 384, 619.
- Wisdom, J., & Holman, M. 1991, *AJ*, 102, 1528
- Wolf, A.S., Laughlin, G., Henry, G., Fischer, D.A., Marcy, G.W., Butler, R.P., Vogt, S. 2007, *ApJ*, 667, 659.
- Wright, J. T., et al. 2007, *ApJ* 657, 533.
- Yu, Q., & Tremaine, S. 2001, *AJ*, 121, 1736
- Zakamska, N.L., Tremaine, S. 2004 128, 869.

TABLE 1
ORBITAL ELEMENTS OF REMAINING PLANET FOLLOWING AN EJECTION

$m_{(2)}/M$	$m_{(1)}/M$	$m_1 = m_{(2)}$		$m_2 = m_{(2)}$		$\langle e_f \rangle$	combined		
		$\langle a_f \rangle$	σ_{a_f}	$\langle a_f \rangle$	σ_{a_f}		σ_{e_f}	$\langle i_f \rangle$ ($^\circ$)	σ_{i_f} ($^\circ$)
0.0012	0.0048	0.933	0.010	0.813	0.006	0.202	0.056	1.93	1.10
0.0015	0.0045	0.888	0.009	0.779	0.005	0.263	0.071	1.99	1.22
0.0018	0.0042	0.828	0.030	0.736	0.047	0.333	0.100	2.22	1.84
0.0021	0.0039	0.749	0.076	0.677	0.083	0.421	0.133	2.94	3.26
0.0024	0.0036	0.670	0.079	0.618	0.085	0.513	0.145	3.80	4.76
0.0027	0.0033	0.595	0.054	0.577	0.053	0.602	0.142	4.23	3.23
0.0030	0.0030	0.573	0.008	0.573	0.008	0.624	0.135	4.696	4.058
0.0003	0.0003	0.537	0.013	0.537	0.013	0.590	0.146	5.319	3.726
0.0005	0.0005	0.543	0.015	0.543	0.015	0.573	0.149	5.615	4.283
0.0010	0.0010	0.552	0.008	0.552	0.008	0.612	0.147	6.304	5.343
0.0020	0.0020	0.565	0.008	0.565	0.008	0.616	0.140	5.204	4.456
0.0030	0.0030	0.573	0.008	0.573	0.008	0.624	0.135	4.696	4.058
0.0050	0.0050	0.586	0.009	0.586	0.009	0.640	0.123	3.802	3.583
0.0100	0.0100	0.598	0.010	0.598	0.010	0.640	0.120	3.119	2.946

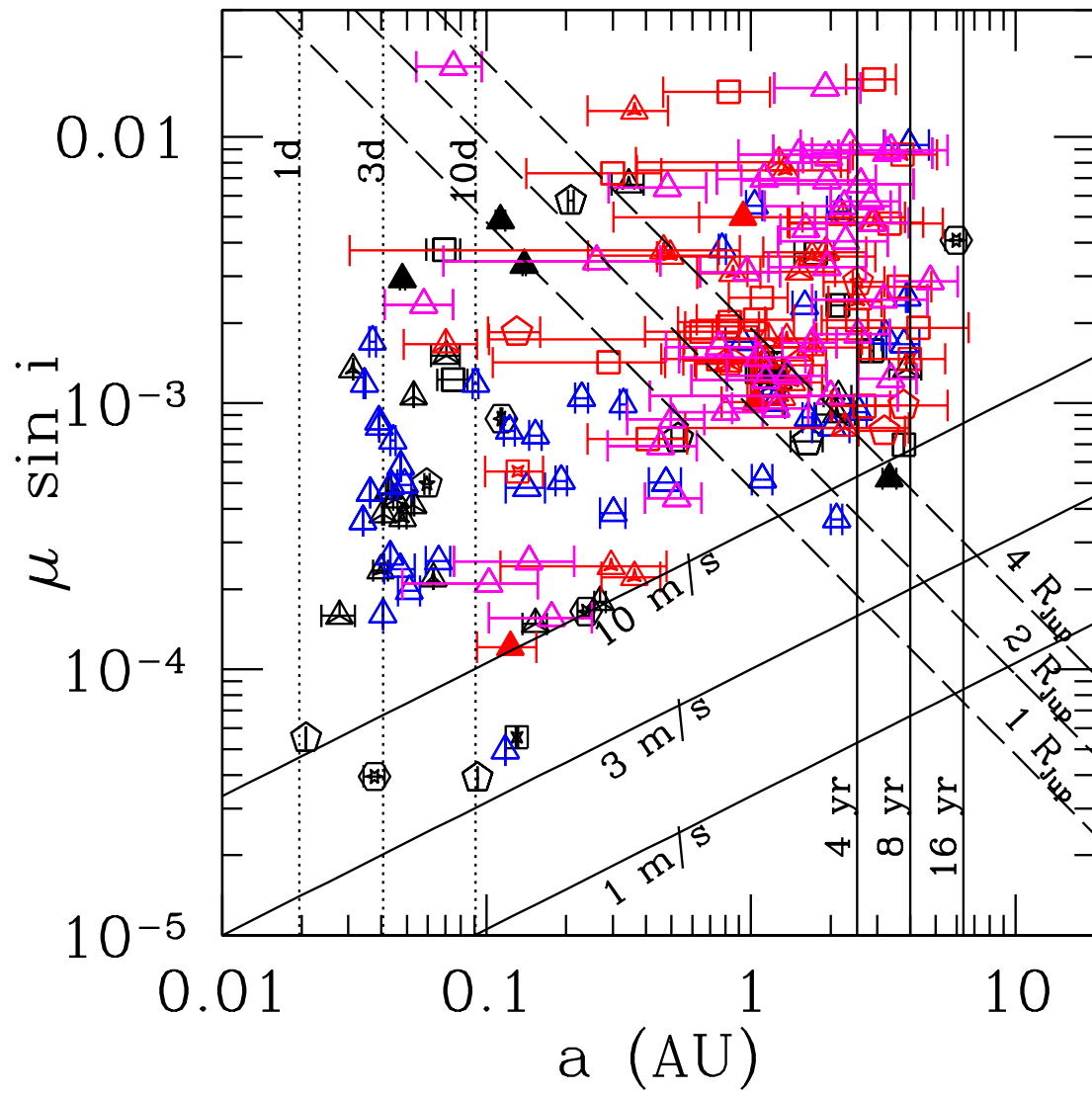


FIG. 1.— Mass Ratio (times sine of inclination of orbital planet to line of sight) versus semi-major axis. Each point corresponds to one planet discovered by radial velocity method, as cataloged by Butler et al. (2006) and updated by Johnson et al. (2006) and Wright et al. (2006). The horizontal bars on each point indicate the periastron and apoastron distances. The solid diagonal lines indicate curves of constant radial velocity semi-amplitude and roughly indicate amplitudes where radial velocity searches lose sensitivity. The solid vertical lines correspond to orbital periods (assuming a stellar mass of $1M_{\odot}$ for which the finite temporal baseline of existing radial velocity surveys limits detection and/or precise measurements of orbital parameters. The dotted vertical lines correspond to orbital periods below which tidal circularization is likely to have damped orbital eccentricities. The dashed diagonal lines correspond indicate curves of constant $\theta^2 \sin i \equiv \mu a \sin i / R_p$, where R_p is the planet radius and R_{Jup} is the radius of Jupiter. Planets with apoastron to the left of this curve are not currently able to efficiently eject other bodies from the planetary system. Open points indicate planets around stars with no known binary companion and no evidence for a long-term radial velocity trend. Points with lines extending from the center to each vertex correspond to planets orbiting a star that also shows a long term radial velocity trend. Points with a star inside correspond to planets orbiting a star in a known stellar binary (Desidera & Barbieri 2006). Solid points correspond to planet orbiting stars with both a stellar binary companion and a long term radial velocity trend. The number of sides for each point equals to the number of known planets orbiting the same star plus two. Black and blue points correspond to planets with current best-fit eccentricities less than 0.2, while red and magenta points correspond to planets with eccentricities greater than 0.2. Blue and magenta points correspond to planets around stars with only one currently known extrasolar planet, no known binary companion, and no evidence for a long-term radial velocity trend. Black and red points correspond to planets orbiting stars that are known to have either two or more planets, a binary companion, or a long-term radial velocity trend. Magenta points to the left of all the diagonal dashed lines correspond to planets for which the eccentricity is unlikely to be explained by planet-planet scattering and there is currently no evidence for additional massive bodies orbiting their host star.

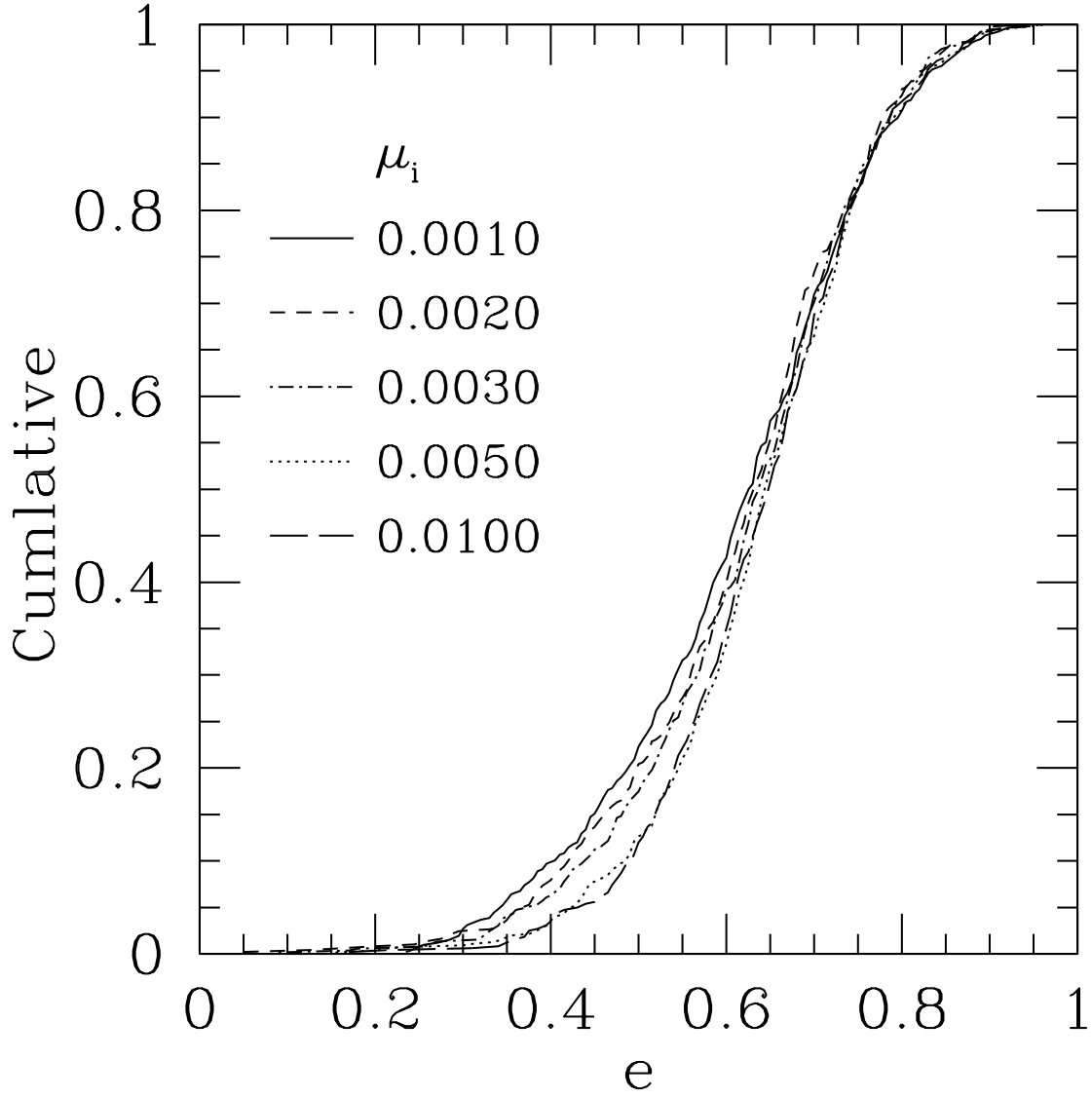


FIG. 2.— Cumulative distributions for the final eccentricity of the remaining planet after the other planet has been ejected. Each line style corresponds to an ensemble of simulations with a different value of $\mu_1 = \mu_2$ as specified in the legend. While the branching ratios for different outcomes depend on the total planet mass, the orbital properties for a given type of outcome (i.e., ejection or collision) are insensitive to the total mass.

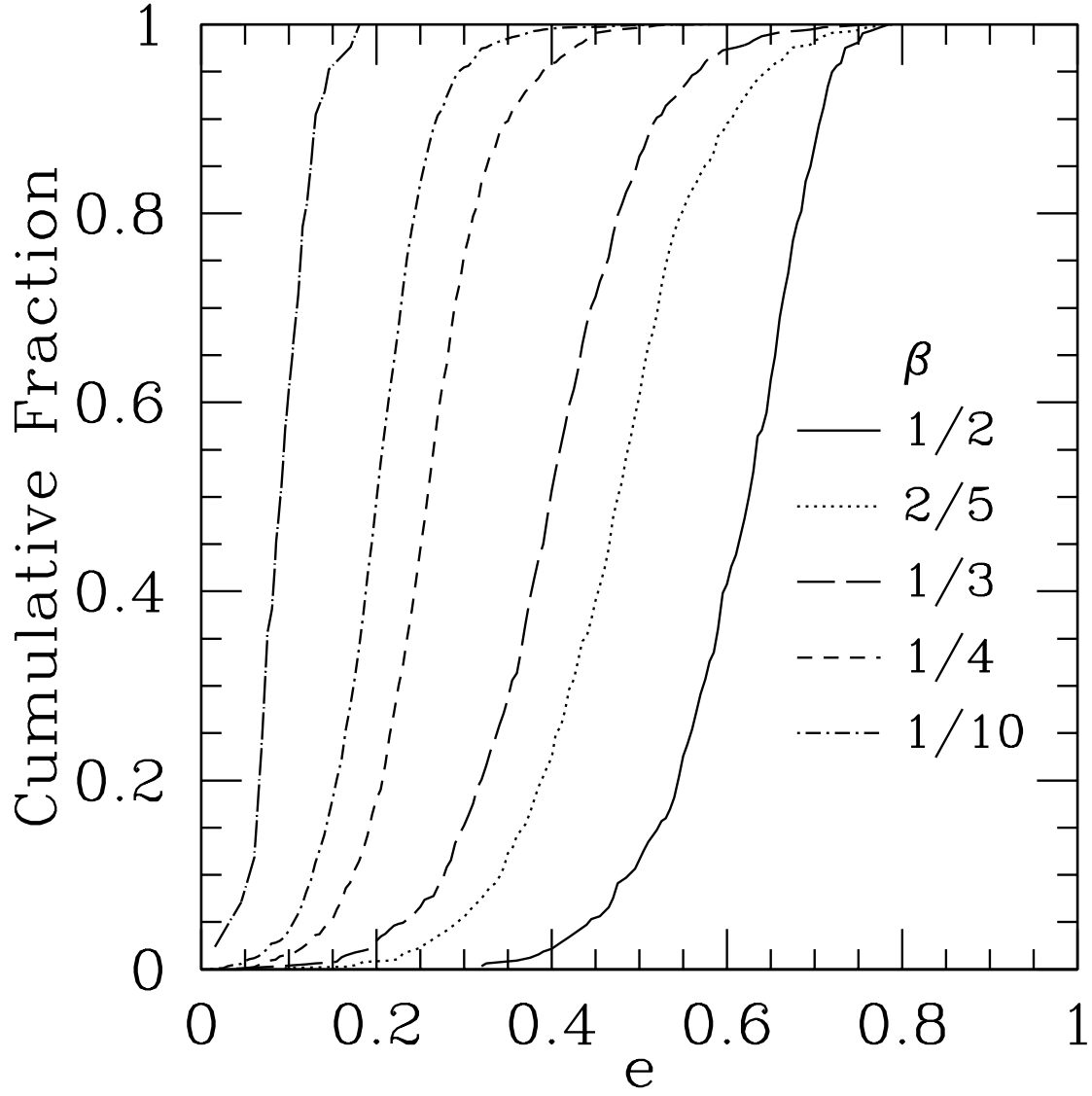


FIG. 3.— Cumulative distributions for the final eccentricity of the remaining planet after the other planet has been ejected. Each line style corresponds to an ensemble of simulations with $\mu_1 + \mu_2 = 6 \times 10^{-3}$ and a different value of $\beta \equiv m_f/(m_1 + m_2)$, where m_f is the mass of the mass of the putative ejected planet.

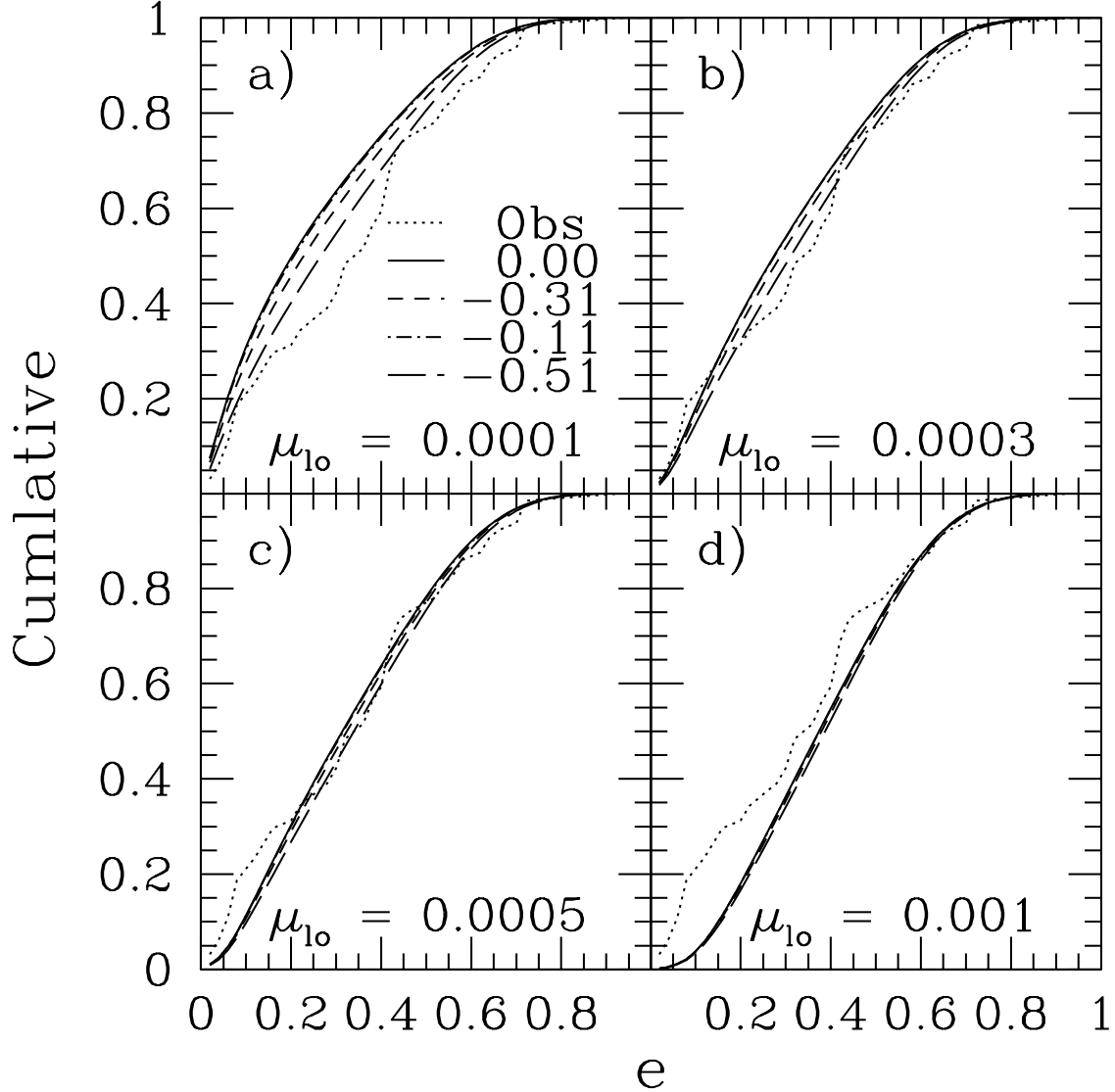


FIG. 4.— Cumulative distributions for the final eccentricity of the remaining planet after the other planet has been ejected. Each line style corresponds to an ensemble of systems with a different power law index for the mass distribution, as indicated in the legend of panel a. The solid line corresponds to an initial distribution uniform in the log of the planet mass. The short dashed curves correspond to best estimate for the planet mass distribution based on the analysis of Cumming et al. 2008. The short-long dashed and dot-dashed curves correspond to the limits of the quoted 1-sigma uncertainty in the power-law index. The dotted curve in each panel corresponds to the observed eccentricity distribution (excluding planets with orbital periods less than 10 days). The different panels correspond to different choices for the cutoff at low masses. Each panel assumes a cutoff of $\mu_{hi} = 10^{-2}$, based on findings of radial velocity surveys.

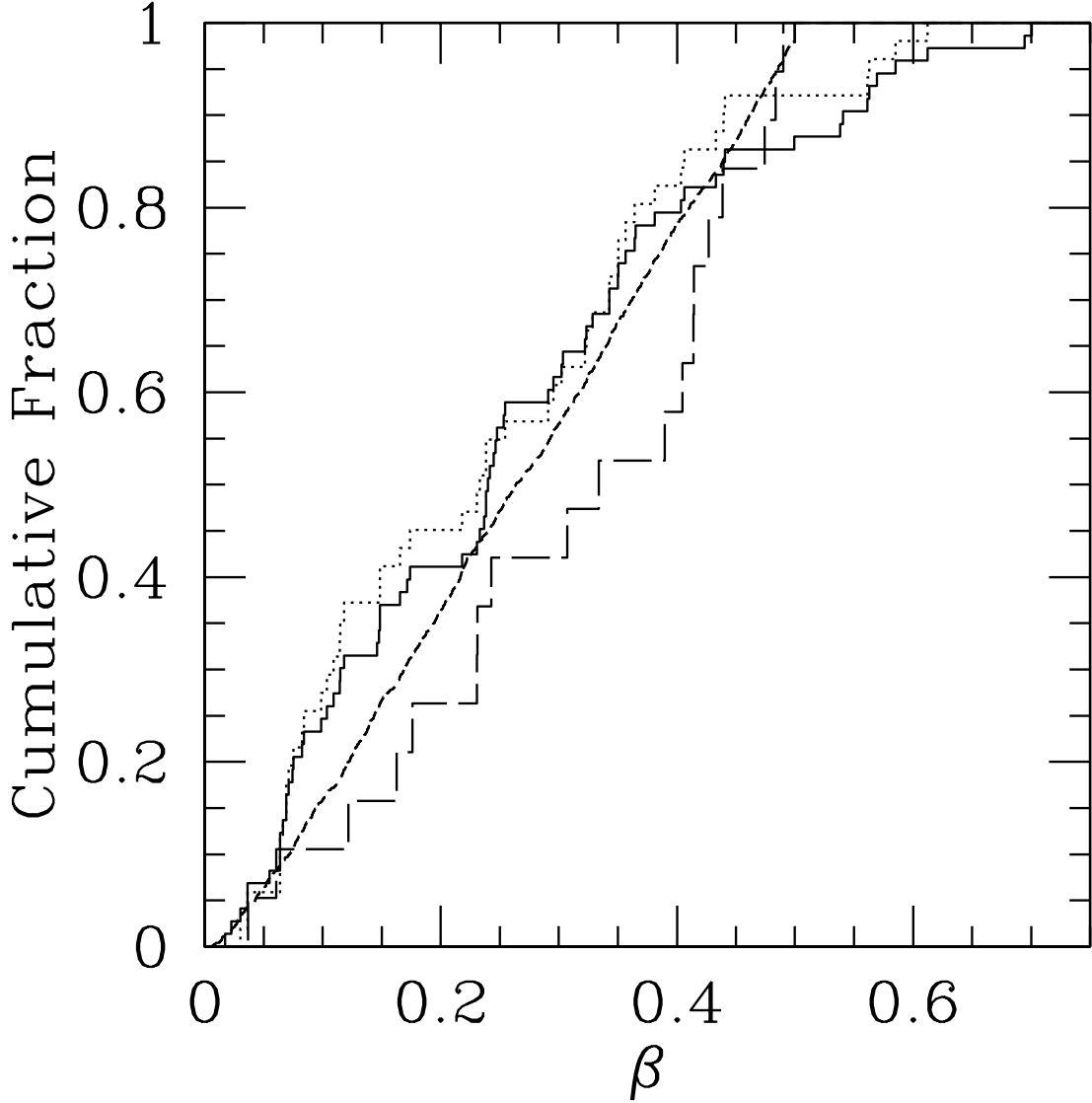


FIG. 5.— Cumulative distributions for β , the ratio of the mass of one planet to the sum of the two planet masses. The solid curve is determined by assuming that the eccentricity of each of the known extrasolar planets (with orbital period between ten days and half the temporal baseline of the published radial velocity observations) is due to planet-planet scattering. The dotted line is similar, but excludes planets in known binary systems. The long dashed line is the distribution of $m_{(2)}/(m_{(1)} + m_{(2)})$ for known multiple planet systems, where $m_{(1)}$ is the most massive planet known to orbit a star and $m_{(2)}$ is the second most massive planet orbit known to orbit the same star (assuming coplanar orbits). The short dashed line is the distribution of β derived by drawing two planet masses (independently and with replacement) from the catalog of extrasolar planets discovered via radial velocity planet searches.

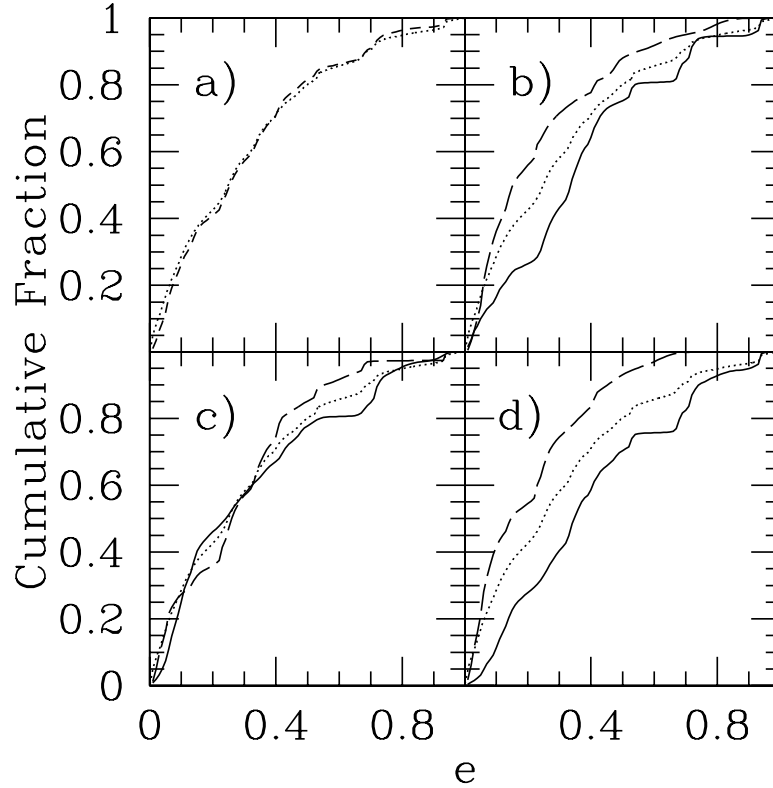


FIG. 6.— Cumulative distributions for eccentricities of known extrasolar planets. Each cumulative distribution is based on the currently known extrasolar planets discovered by radial velocity surveys with orbital period between ten days and half the temporal baseline of the published radial velocity observations. A few planets have been omitted due to significant uncertainty in the eccentricities (§4.3). The short-dashed curve in panel a is based on the published best-fit eccentricities and uncertainties. The dotted curves (repeated in each panel) are based on a Bayesian analysis of the published radial velocity observations for each planetary system (Butler et al. 2006, Johnson et al. 2006, Wright et al. 2006). In panels b-d, we repeat this analysis for two subsets of this sample. In panel b, the solid (dashed) curve is for planets with $m \sin i$ greater (less) than $1.57 M_J$. In panel c, the solid (dashed) curve is for planets with an orbital period greater (less) than 350d. In panel d, the solid (dashed) curve is for planets with $\theta^2 \sin i$ greater (less) than 1.69, where θ is the ratio of the escape velocity from the planet (evaluated at its surface) to the escape velocity from the sun (evaluated at the planet’s apastron). The threshold values of $m \sin i$, period, and θ were chosen to result in sample sizes as nearly equal as possible.

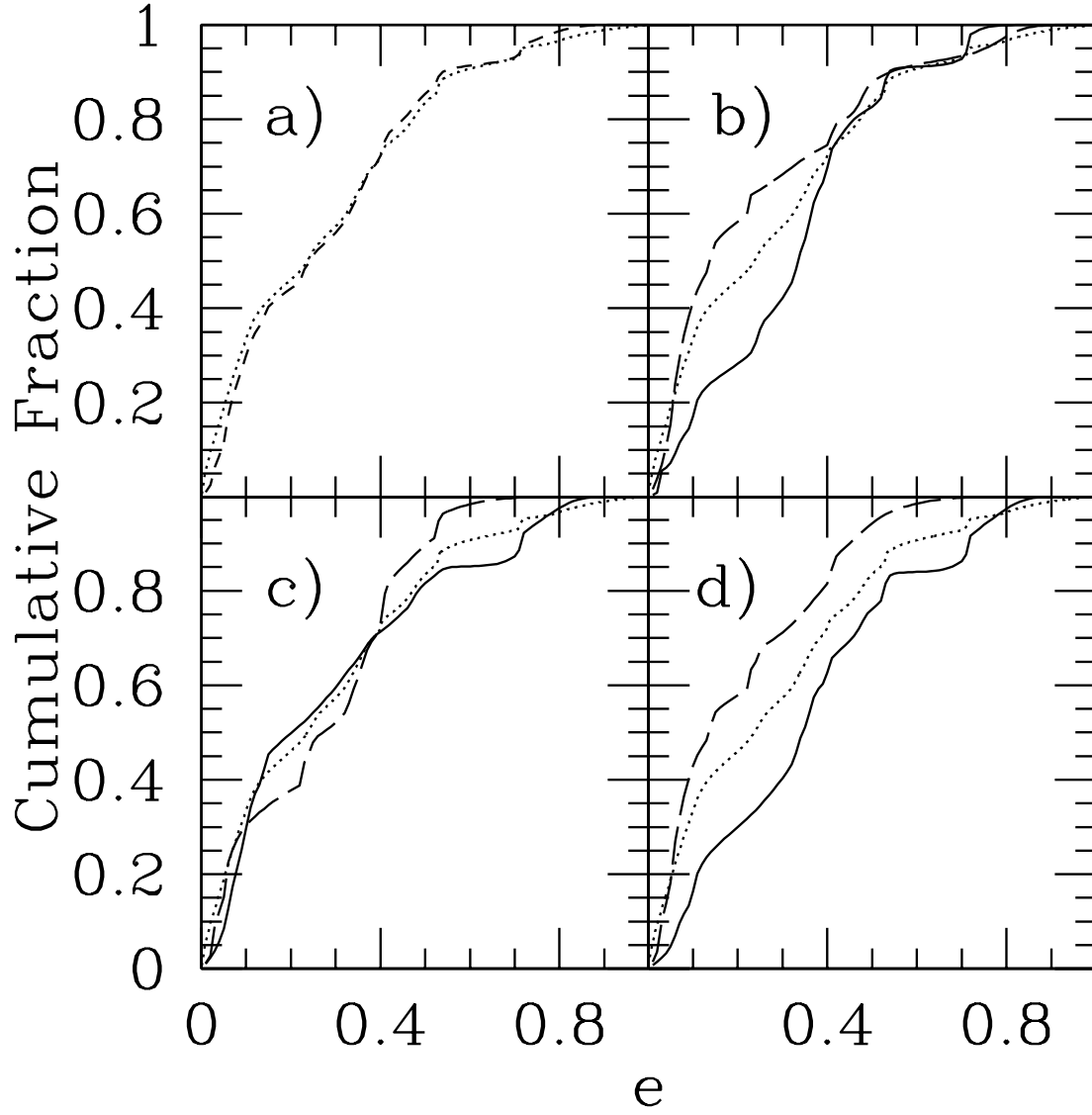


FIG. 7.— Cumulative distributions for eccentricities of known extrasolar planets not in a known binary system. Same as Fig. 4, except only for planets that are not part of a known binary star system.

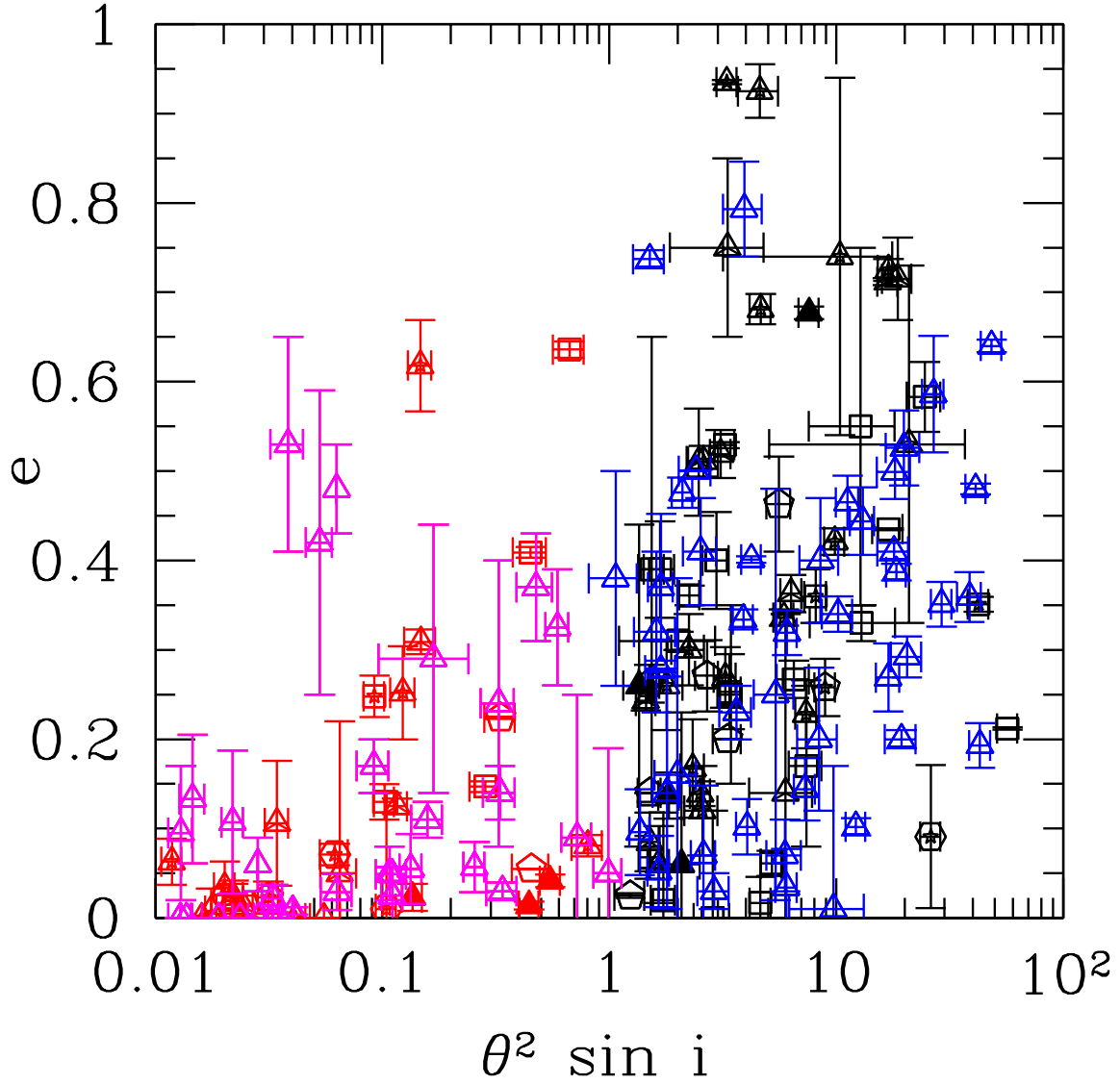


FIG. 8.— Ratio of the escape velocity from the planet to the escape velocity from the sun (θ^2) versus eccentricity. Each point corresponds to the best-fit solution and uncertainty published in Butler et al. (2006), as updated by Johnson et al. (2006) & Wright et al. (2006). The planet radius is estimated using the models of Bodenheimer et al. (2003). The horizontal error bar assumes that the planet radius is known precisely. The point styles and colors are the same as in Fig. 1.